



Cite this: DOI: 10.1039/d5fb00791g

# Chitosan-coated nanoemulsions loaded with lemongrass essential oil: formulation and process optimization for postharvest quality retention and shelf-life extension of papaya

Dharini Venkatachalam,<sup>a</sup> Periyar Selvam Sellamuthu,<sup>ID</sup> \*<sup>a</sup> Jayaramudu Jarugala<sup>b</sup> and Sadiku Emmanuel Rotimi<sup>ID</sup> <sup>c</sup>

Papaya fruits are highly susceptible to rapid postharvest deterioration, leading to substantial economic losses. This study aimed to develop an optimized chitosan-coated nanoemulsion (CC-NE) based functionalized coating by integrating bioactive lemongrass essential oils (LGEOs) into biopolymeric carriers to provide controlled release properties for extending the shelf-life of papaya. The effects of chitosan (0.5–1.5%), gum arabic (1–3%) and dispersed oil phase (0.01–0.15%) concentrations on the particle size, zeta potential, polydispersity index, and antifungal activity against *Lasiodiplodia theobromae* and *Rhizopus stolonifer* were evaluated by employing a Box–Behnken response surface methodology. The optimized formulation (0.5% chitosan, 2.5% gum arabic and 0.07% dispersed oil phase) produced a stable nanoemulsion with high encapsulation efficiency (87.4%) and excellent thermodynamic stability. The morphological analysis revealed spherical droplets with a uniform core–shell structure, indicating successful encapsulation of LGEO with the stabilized chitosan matrix. Further characterization revealed low viscosity, reduced turbidity and enhanced whiteness index properties, suggesting superior visual and functional properties. The shelf-life studies demonstrated that CC-NE coated papayas exhibited significantly lower weight loss (23.9%), delayed firmness reduction, slower peel colour changes, and controlled biochemical changes compared to the untreated control and fungicide-treated control groups. Moreover, the sensory evaluation confirmed superior colour, texture, aroma, and overall acceptability of the CC-NE treated fruits after 14 days of ambient storage. The findings ensure the CC-NE as a safe and effective alternative to synthetic fungicides, with strong potential for application in sustainable fruit coating and storage systems.

Received 30th October 2025  
Accepted 8th March 2026

DOI: 10.1039/d5fb00791g

rsc.li/susfoodtech

## Sustainability spotlight

(1) This study presents an eco-friendly formulation that uses chitosan and gum arabic as renewable and biodegradable biopolymers for natural coating applications. (2) The work applies green nanotechnology through a nanoemulsion system that efficiently delivers lemongrass essential oil and reduces the dependence on synthetic fungicides. (3) The formulation ensures food safety by providing residue-free preservation and minimizing chemical exposure to consumers. (4) The use of bio-derived materials lowers environmental impact and replaces petroleum-based coatings with sustainable alternatives. (5) This approach supports economic sustainability by helping smallholder fruit producers retain product quality and market value during storage and distribution. (6) The work aligns with global sustainability goals promoting food security, responsible production, and climate resilience.

## Introduction

Postharvest losses of fruits and vegetables pose a major threat to global economic development, food security and sustainability. Developing countries, particularly those in warm and humid climatic zones, are prone to major postharvest losses of fruits and vegetables, ranging from 28 to 55% of total production,<sup>1</sup> leading to a considerable waste of nutritional resources. Among these, papaya (*Carica papaya* L.) is known for its rapid ripening and senescence once harvested, marking it as a highly perishable climacteric fruit. As a result, significant physiological and biochemical changes render it susceptible to microbial decay,

<sup>a</sup>Department of Food Technology (Formerly Food Process Engineering), Postharvest Research Lab, School of Bioengineering, SRM Institute of Science and Technology, Potheri, Kattankulathur, Chengalpattu District, Tamil Nadu, 603203, India. E-mail: periyars@srmist.edu.in; periyar.india@gmail.com

<sup>b</sup>Polymer and Functional Materials Division, CSIR-Indian Institute of Chemical Technology (IICT), Uppal Road, Tarnaka, Hyderabad, 500007, India

<sup>c</sup>Institute of NanoEngineering Research (INER), Department of Chemical, Metallurgical and Materials Engineering, Tshwane University of Technology, Pretoria West Campus, Staatsartillerie Rd, Pretoria, 0183, Republic of South Africa



hastening the deterioration under ambient storage conditions. Fruits undergo rapid weight loss, nutrient degradation, fungal decay, softening and discolouration of peel in less than one week in uncontrolled storage environments.<sup>2,3</sup>

Conventional methods, such as using synthetic fungicides and chemical preservatives, have been widely employed for controlling postharvest fungal decay to delay spoilage and extend shelf-life. However, these approaches yield concerns related to food safety and chemical residues, a potential threat to the environment and the food chain.<sup>4</sup> In this regard, the search for safer, eco-friendly and sustainable preservation technologies has intensified in recent times. One of the promising approaches is the use of natural biopolymers and bioactive compounds as an edible coating on the surface of fruits. Recently, postharvest losses on berries<sup>5</sup> and strawberries<sup>6</sup> were significantly controlled through effective fruit coating technologies. These coatings act as a semipermeable membrane by reducing the loss of moisture and controlling the gaseous exchange and physiological processes associated with ripening.<sup>7</sup> However, their direct application in the food system is limited by volatility, hydrophobicity and instability under storage conditions. To overcome these limitations, nanoemulsion (NE) technology offers a viable strategy by enhancing the solubility, stability, bioavailability and controlled release of active agents in the coating formulation.<sup>8</sup> The NE system consists of two immiscible liquids (oil phase and aqueous phase) and an emulsifier.<sup>9</sup> Hydrophobic compounds have been effectively delivered using the NE system, which disperses the lipid phase as a colloidal dispersion.<sup>10</sup> Among hydrophobic bioactive compounds, essential oils are widely incorporated as active functional agents in coating systems. Essential oils (EOs) are recognized for their potent antifungal and antibacterial properties.<sup>11</sup> Among these, recent studies have shown that lemongrass essential oil (LGEO) effectively inhibits pathogenic fungi such as *Rhizopus*, *Aspergillus* and *Lasiodiplodia*, the major postharvest pathogens of tropical fruits.<sup>12,13</sup> Despite its potential, direct application of LGEO is hindered by rapid volatilization, poor water solubility, and susceptibility to degradation. To overcome these limitations, the EO should be encapsulated with biopolymers to provide structural integrity and controlled delivery.<sup>14</sup> While encapsulating LGEO into a nanoemulsion system, polysaccharides are the most preferred carrier materials for the effective delivery of its bioactive components.<sup>15,16</sup> The various advantages include bioavailability, biodegradability and cost-effectiveness.<sup>17</sup> Chitosan (CH), the cationic polymer, is an excellent non-toxic source for encapsulating EO to improve its antimicrobial properties. Several studies prove that CH was effective in encapsulating spearmint EO<sup>18</sup> and lemon EO<sup>19</sup> for extending the storage life of citrus fruits and grapes, respectively. The ultimate success of an effective NE system lies in the potential release of EO over extended periods, offering microbial growth inhibition.<sup>20</sup> Likewise, gum arabic (GA) is an amphiphilic polysaccharide with good emulsifying properties capable of forming complexes through electrostatic interactions. The study by Zhang *et al.* (2022)<sup>21</sup> has demonstrated that CH/GA complexes can form a stable emulsion with enhanced particle delivery under various environmental stresses. A

similar study by Han *et al.* (2020)<sup>22</sup> reported that CH/GA complexes were effective in forming a stable emulsion with enhanced delivery of curcumin-based bioactive materials.

Recent studies have demonstrated that NE-based coatings containing essential oils significantly enhance postharvest quality and delay spoilage in tropical fruits. More specifically, in papaya fruits, thyme oil NE coatings improved the shelf-life and storage quality for up to 10 days.<sup>23</sup> Likewise, carnauba wax-based NEs containing ginger EO had retained the storage shelf-life by reducing the respiration rates and delaying the ripening of papaya fruits.<sup>24</sup> Similarly, a study by Oliveira Filho *et al.* (2022)<sup>25</sup> revealed that carnauba wax-based NE coating containing palmarosa EO sustained the overall quality parameters for 12 days, reducing the incidence and severity of postharvest diseases in papaya fruits. Consequently, spearmint and clove EO-based NE coatings applied to papaya fruits delayed fruit rot, controlled ripening and retained postharvest fruit quality.<sup>26</sup> Corresponding to papaya fruits, NE coatings incorporated with clove and peppermint EOs significantly reduced the postharvest losses and improved the commercial viability of lychee fruits.<sup>27</sup> A study by Tafa *et al.* (2025)<sup>28</sup> involved pectin-rosemary EO-based NE coating of apple and banana fruits. A significant improvement in the quality attributes was observed for the NE-coated fruits. Compared to previously reported essential oil-based NE coatings, chitosan-coated nanoemulsions (CC-NEs) demonstrated enhanced physicochemical stability and preservation efficacy while offering improved cost-effectiveness due to their biopolymer-based formulation and reduced reliance on volatile essential oils. Chitosan-entrapped EO-based NEs have proven to enhance stability, sustain preservation efficacy, improve interfacial stability, and control the release of active compounds.<sup>29</sup> In addition, the aqueous-based CC-NE formulation utilizes inexpensive, commercially available biopolymers, indicating favourable economic feasibility for large-scale postharvest applications. These attributes highlight the potential of CC-NEs as a scalable and sustainable postharvest coating technology for fruits.

The formulation of an effective coating solution involves a tedious optimization process to ensure the desired characteristics. This includes selecting the appropriate chitosan, gum arabic and dispersed oil phase concentration to attain a coating solution with stable efficacy. Response Surface Methodology (RSM) is a powerful mathematical modelling tool for evaluating the effects of multiple factors and their interactions on the desired responses,<sup>30</sup> such as particle size, zeta potential, polydispersity index, and antifungal activity against *Lasiodiplodia theobromae* and *Rhizopus stolonifer*. Several pieces of evidence from recent studies employed the Box–Behnken design for the optimization of stable NE systems used in the surface coating of fruits.<sup>31,32</sup> While several studies have explored nanoemulsion-based edible coatings, a significant gap remains. Most research has focused on single biopolymer matrices or conventional emulsions, with limited work on nanostructured chitosan-coated systems. Moreover, systematic optimization of NE parameters of the nanoscale droplets and their antifungal properties has not been extensively applied to papaya. Similarly, there is limited information on how optimized chitosan-coated



NE systems influence the physicochemical attributes of papaya fruits during extended storage. Addressing these gaps is essential for advancing the application of these coatings in commercial postharvest management. Therefore, this study aims to investigate the optimal conditions of the process variables that maximize the beneficial effects of the responses in chitosan-coated nanoemulsion-based coating solutions loaded with lemongrass essential oil. The effectiveness of the optimized coating solution was analysed through shelf-life studies on fresh papaya fruits.

## Materials and methods

The papaya fruits for the shelf-life studies were sourced from a central market in Koyambedu, Tamil Nadu, India. The fruits were selected based on their uniform size ( $700 \pm 100$  g) with a colour index of two (green stripe with a slight trace of yellow), free from surface damage and pathogenic infection. Chitosan and gum arabic (food grade) were purchased from Sisco Research Laboratories Pvt Ltd (SRL), Mumbai, India. Lemongrass (*Cymbopogon citratus* L.) essential oil was purchased from Cyrus Enterprises, Chennai, Tamil Nadu, India. All other reagents used in the experiments were of analytical grade and stored at  $25 \pm 2$  °C.

### Formulation of chitosan-coated nanoemulsion solution

Formulation of the Chitosan-Coated Nanoemulsion (CC-NE) is a two-step process. Generally, an emulsion is a solution containing a dispersed and continuous phase. The oil-in-water emulsion is one of its types, where the dispersed phase is an oil medium and the continuous phase is water.

**Preparation of the dispersed phase (DP).** The dispersed phase contains lemongrass essential oil (LGEO) and sunflower oil in a ratio of 1:1, mixed with 0.5 wt% of Tween 80 surfactants. The sunflower oil was added to prevent coalescence and Oswald ripening. The ratio of LGEO to sunflower oil was fixed based on the previous trials to check the stability against phase separation. The mixture was continuously stirred for 1 h in a magnetic stirrer. This mixture of DP was added at different concentrations (0.01–0.15% v/v) to the continuous phase.

**Preparation of a CC-NE.** GA solution was prepared by adding the respective quantities (1–3% w/v) in distilled water. The solution was stirred with a magnetic stirrer for 60 min at 40 °C and filtered to remove impurities.<sup>33</sup> The DP at different concentrations (0.01–0.15% v/v) was added to the GA (1–3% w/v) solution and stirred for 1 h using a magnetic stirrer. The coarse emulsion was then mixed with CH (0.5–1.5% w/v) solution and homogenized for 15 min. The resultant mixture was placed in an ice water bath and sonicated with an ultra-probe sonicator<sup>34</sup> for 10 min to obtain a CC-NE.

### Experimental design and methodology

The effects of three process variables CH ( $X_1$ ), GA ( $X_2$ ) and DP ( $X_3$ ) on various responses were evaluated in terms of particle size ( $Y_1$ ), zeta potential ( $Y_2$ ), polydispersity index (PDI) [ $Y_3$ ] and antifungal activity against *L. theobromae* ( $Y_4$ ) and *R. stolonifer*

Table 1 Experimental design for various parameters

Run	Chitosan (%)	Gum arabic (%)	Dispersed phase (%)
1	1	2	0.08
2	0.5	3	0.08
3	1	3	0.15
4	1	3	0.01
5	0.5	1	0.08
6	1.5	3	0.08
7	1	1	0.01
8	1	1	0.15
9	1	2	0.08
10	1.5	1	0.08
11	1	2	0.08
12	1	2	0.08
13	0.5	2	0.01
14	1.5	2	0.01
15	1.5	2	0.15
16	0.5	2	0.15
17	1	2	0.08

( $Y_5$ ). A three-level (−1, 0, +1) and three-factor Box–Behnken Design (BBD) with five centre point replications was applied to study the effects of process parameters  $X_1$ ,  $X_2$  and  $X_3$ . The ranges of the variables for the preparation of CC-NE solutions are shown (Table 1). A total of 17 runs were generated, among which five runs were centre points. The centre point runs were performed five times to determine the errors resulting from BBD. The experiments were performed in triplicate for all the trials in the RSM design (Design Expert, version 7.0.0; State-Ease Inc., USA). The generated second-order polynomial equation of the response is as follows:

$$Y = b_0 + b_1X_1 + b_2X_2 + b_3X_3 + b_{12}X_1X_2 + b_{13}X_1X_3 + b_{23}X_2X_3 + b_{11}X_1^2 + b_{22}X_2^2 + b_{33}X_3^2 \quad (1)$$

In eqn (1),  $Y$  denotes the response and  $b_0$  is a constant regression coefficient.  $b_1$ ,  $b_2$  and  $b_3$  are linear coefficients. Likewise,  $b_{12}$ ,  $b_{13}$ ,  $b_{23}$  are interaction coefficients and  $b_{11}$ ,  $b_{22}$ ,  $b_{33}$  are the coefficients of the quadratic terms.  $X_1$ ,  $X_2$  and  $X_3$  represent the process variables.

### Characterization of the optimized chitosan coated nanoemulsion solution

The optimized CC-NE solution was characterized further to study its morphology, viscosity, turbidity, whiteness index, encapsulation efficiency and thermodynamic stability. Here, three different solutions are subjected to characterization for comparison and better understanding. The first solution is the coarse emulsion of the oil phase mixed within the phosphate buffer solution. The second solution is the primary emulsion prepared by adding a stabilizer to the oil phase. The third solution is the optimized CC-NE solution. Henceforth, the coarse emulsion solution contains LGEO and sunflower oil in a ratio of 1:1 mixed with 0.5 wt% of Tween 80 surfactants to 100 mL of phosphate buffer solution. The mixture was continuously stirred for 1 hour using a magnetic stirrer. The primary NE solution was prepared by adding the oil phase to the GA



stabilizer solution, followed by continuous stirring for 6 hours. Finally, the CC-NE solution was prepared according to the optimized results obtained from the RSM. The solution containing 0.5% CH, 2.5% GA and 0.07% oil phase concentrations was subjected to homogenization and ultrasonication processes to obtain the CC-NE.

**Morphological analysis.** The morphology of the coating solutions was studied using a Transmission Electron Microscope (TEM). The samples were diluted in a ratio of 1 : 10 using distilled water and deposited onto copper grids (250 mesh square grid). Excess solution was removed using filter paper, and the samples were allowed to dry for 12 hours. The images of all the dried samples were captured through TEM (JEM-2100 Plus, JEOL Japan) analysis.

**Viscosity.** The viscosity of the coating solutions was determined using a Brookfield digital viscometer (DV-II Plus Pro) at  $25 \pm 2$  °C. The experiment was performed using 10 mL of the coating solution with spindle number 64 at an average speed of 60 rpm, and the results were expressed in mPa s.<sup>35</sup> Each experiment was performed with three replicates, and the results were tabulated.

**Turbidity.** The measurement of turbidity was done according to the method performed by Basak and Guha (2017)<sup>36</sup> with slight modifications. The absorbance of all the coating solutions was measured at a 600 nm wavelength. Each experiment was performed with three replicates, and the results were tabulated.

**Whiteness index.** The colour of the coating solution was measured using a Hunter ColorQuest XE colourimeter (A60-1011-610, Hunter Lab, Virginia, USA) calibrated with a standard white plate.<sup>37</sup> The whiteness index was calculated with eqn (2).

$$\text{Whiteness index} = 100 - ((100 - L)^2 + (a^2 + b^2))^{0.5} \quad (2)$$

**Measurement of encapsulation efficiency and loading capacity.** The encapsulation efficiency (EE) and loading capacity (LC) were analysed by UV-visible spectrophotometry according to the procedure of Deepika *et al.* (2021)<sup>38</sup> with slight modifications. About 100  $\mu$ L of the formulated NEs were mixed with 3 mL of ethanol. The samples were centrifuged at 10 000 rpm for 10 min. The amount of LGEO in the supernatant was determined at a wavelength of 235 nm. The pure LGEO prepared with ethanol was used to construct a standard curve ( $R^2 = 0.999$ ). The emulsions without the addition of LGEO, prepared in the same manner, were used as a blank. The EE and LC were calculated in percentage with the equation given below.

$$\text{EE}\% = \frac{\text{Absolute amount of loaded LGEO}}{\text{Total amount of LGEO taken}} \times 100 \quad (3)$$

$$\text{LC}\% = \frac{\text{Absolute amount of loaded LGEO}}{\text{Weight(mg)of formulated nanoemulsions}} \times 100 \quad (4)$$

**Thermodynamic stability studies.** The stability of the prepared emulsions was analysed by subjecting them to different conditions, such as centrifugation, moderate heating and refrigeration to study the phase separation of the emulsions. After

a storage period of 24 hours, phase separation was observed in the emulsion with the formation of a less dense upper layer and a denser lower layer. The phase separation was calculated in terms of the Creaming Index (CI) using the following equation:<sup>39</sup>

$$\text{CI} = \frac{H_t}{H_0} \times 100 \quad (5)$$

Here,  $H_t$  is the height of the creamed layer after 24 hours and  $H_0$  is the initial height of the emulsion.

**Centrifugation stability.** The emulsions were centrifuged (Remi, C - 24 Plus) at 10 000 rpm for 30 min. Following centrifugation, the samples were left undisturbed for 24 hours at room temperature and checked for phase separation.<sup>36</sup>

**Heating/freezing stability.** The emulsions were subjected to moderate heat of 40 °C for 10 min and stored at room temperature for 24 hours. Phase separation was noted at the end of this period. To analyse the freezing stability, the different emulsion formulations were stored at  $-10$  °C for 24 hours and observed for phase separation.<sup>36</sup>

### The CC-NE treatments on fresh papaya fruits

In the formulation of the CC-NE coating solution, 0.5% (w/v) of CH was dissolved in aqueous acetic acid solution (1% v/v), followed by overnight stirring to obtain the complete dispersion of chitosan powder.<sup>40</sup> A gum arabic solution was prepared by adding 2.5% (w/v) of the GA mixture in distilled water. After 60 min of stirring at 40 °C with a magnetic stirrer, the mixture was filtered to get rid of any impurities.<sup>33</sup> The concentration of the DP to be added to the continuous phase was based on the results obtained from the optimization studies. The DP was added at 0.07% (v/v) to the GA solution and stirred for 1 hour using a magnetic stirrer. The coarse emulsion was then mixed with CH solution and homogenized for 15 min, and the resultant mixture was placed in an ice water bath and sonicated with an ultra-probe sonicator<sup>34</sup> for 10 min to obtain a CC-NE. To perform this study, five different treatments were used. They are control (without any coating), carbendazim coating (Carb), CH + DP coating, GA + DP coating and CC-NE coating. The carbendazim coating was used as a positive control. Each treatment was performed with three replicates, consisting of three fruits per replication, a total of forty-five fruits. Based on the prior experiments done in the laboratory,<sup>12</sup> papayas were coated by the dipping method and allowed to air dry for 20 min. Both the control and treated fruits were stored in open plastic trays under ambient conditions of  $25 \pm 2$  °C.

### Shelf-life studies on the freshly coated papaya fruits

Before the coating treatments, the fruits were washed with distilled water, surface sterilized with 70% ethanol, allowed to dry in air and stored at  $25 \pm 2$  °C. Physical quality characteristics such as weight loss, firmness and colour values of the fruits were regularly monitored in specific intervals of 0, 4, 8, 12 and 14 days during the entire days after storage (DAS) period. Biochemical quality characteristics, such as total soluble solids, titratable acidity and pH of the fruits, were also monitored at specific periods during the entire storage period using the standard operating procedures performed in the laboratory.<sup>12</sup>



Three replicates per treatment were performed for each analysis, and the results were tabulated.

### Physical quality characteristics

The physical quality parameters of the papaya fruits during the postharvest storage, the firmness value, weight loss and colour parameter of the fruits were regularly monitored in specific intervals of four days during the entire DAS period under ambient conditions of  $25 \pm 2$  °C.<sup>41</sup> A TA-XT texture analyser (Stable Microsystem Ltd, UK) was used to evaluate the fruit's firmness. Measurements were taken from three equatorial regions on both sides of the fruit, yielding nine readings per sample. A 2 mm diameter cylindrical probe was employed, and the results were expressed in units of force, Newton (N). The Hunter colourimeter – ColorQuest XE (A60 – 1011 – 610, Hunter Lab, Virginia, USA) was used to measure the colour of the fruits. The colour values were recorded in the equatorial region, and the “b\*” value in the reading gives the yellowness of the fruit, as the colour is prone to change with the ripeness of the fruit.<sup>42</sup> The papaya fruits were measured for weight using a digital weighing balance (Infra Digi Laboratories, India) in the respective intervals of 0, 4, 8, 12 and 14 days. For each treatment group, the fruits were weighed individually, and the percentage of weight loss was determined using eqn (6).

$$\text{Weight loss(\%)} = \frac{\text{Initial weight} - \text{Final weight}}{\text{Initial weight}} \times 100 \quad (6)$$

### Biochemical quality characteristics

The total soluble solids (TSS) of the sample were measured using a hand-held refractometer (ERMA, Tokyo, Japan), and the results were expressed in °Brix. For measuring the titratable acidity (TA), the papaya samples were titrated against standardized 0.01 N NaOH.<sup>43</sup> The result was expressed as the malic acid percentage. The analysis of pH was done by using a pH

meter (Susima, MP-1 Plus, India), where the electrode was inserted into a beaker containing a papaya sample. The analysis was repeated thrice.<sup>44</sup>

**Antifungal activity.** The antifungal activity on the fruit surface was measured in terms of disease incidence and severity of fruit rot and stem-end rot diseases. The severity percentage of the diseases was assessed based on the visual rating scores.<sup>45</sup> Interpretation of visual scores: 1 represents less than 10% of infection; 2 represents 11 to 25% of disease infestation; 3 represents 26 to 50% of disease infestation; 4 represents 51 to 75% of disease infestation; and 5 represents 76 to 100% of disease infestation. The disease incidence percentage was calculated using the method of Sellamuthu *et al.* (2013)<sup>46</sup> and eqn (7).

$$\text{Disease incidence (\%)} = \frac{\text{Number of infected wounds}}{\text{Total number of wounds}} \times 100 \quad (7)$$

**Sensory evaluation.** The quality of papaya fruit in terms of taste, aroma, colour, texture and overall acceptability was examined. The sensory analysis was performed with a semi-trained panel of thirty members. Fruits from each treatment were sliced, served on plates, and presented in a randomized order. Assessments were carried out using the 9-point Hedonic scale, where 1 denoted extreme dislike and 9 indicated strong liking preference.

**Statistical analysis.** All data were presented as mean  $\pm$  standard error of replicates. Experiments were performed in triplicate, and statistical evaluation was conducted using analysis of variance (ANOVA). Mean differences were further compared using Duncan's multiple range test at a significance level of  $P < 0.05$  with SPSS software (version 19).

## Results and discussion

### Design analysis and fitting the proposed model

The influence of process variables – CH ( $X_1$ : % w/v), GA ( $X_2$ : % w/v), and DP ( $X_3$ : % v/v) concentrations on the responses of particle size

Table 2 The process parameters and responses of Box–Behnken design

Run	Chitosan (%) $X_1$	Gum Arabic (%) $X_2$	Dispersed phase (%) $X_3$	Particle size (nm) $Y_1$	Zeta potential (mV) $Y_2$	Polydispersity index $Y_3$	Antifungal activity against <i>L. theobromae</i> $Y_4$	Antifungal activity against <i>R. stolonifer</i> $Y_5$
1	1	2	0.08	266.6	24.4	0.183	93.2	90.3
2	0.5	3	0.08	249.3	23.8	0.124	98.2	97.1
3	1	3	0.15	430.5	29.5	0.529	72.7	85.8
4	1	3	0.01	361.2	32.2	0.25	69.7	61.4
5	0.5	1	0.08	438	22.8	0.264	90.4	86.6
6	1.5	3	0.08	492.9	25.1	0.412	88.6	87.7
7	1	1	0.01	301.8	34.5	0.203	60.8	61.9
8	1	1	0.15	485	26.5	0.552	85.2	82.7
9	1	2	0.08	265.6	24.4	0.183	93.2	90.3
10	1.5	1	0.08	312.2	24.7	0.251	95.1	95.5
11	1	2	0.08	266.1	24.4	0.183	93.2	90.3
12	1	2	0.08	264.6	24.4	0.183	93.2	90.3
13	0.5	2	0.01	251.3	34.3	0.123	66.2	58.3
14	1.5	2	0.01	302.6	33.1	0.266	70.8	65.1
15	1.5	2	0.15	438.5	30.3	0.591	72.3	85.6
16	0.5	2	0.15	358	27.8	0.442	84.5	87.5
17	1	2	0.08	264.6	24.4	0.183	93.2	90.3



Table 3 ANOVA table specifying the responses for the process variables

Source	Particle size (nm)		Zeta potential (mV)		PDI		Antifungal activity against <i>Lasiodiplodia theobromae</i> (%)		Antifungal activity against <i>Rhizopus stolonifer</i> (%)	
	Sum of squares	<i>p</i> -Value prob > <i>F</i>	Sum of squares	<i>p</i> -Value prob > <i>F</i>	Sum of squares	<i>p</i> -Value prob > <i>F</i>	Sum of squares	<i>p</i> -Value prob > <i>F</i>	Sum of squares	<i>p</i> -Value prob > <i>F</i>
Model	120 034.81	<0.0001	258.24	<0.0001	0.378913	<0.0001	2295.81	<0.0001	2526.5	<0.0001
$X_1$	7787.52	<0.0001	2.53	0.0019	0.4019	<0.0001	19.53	0.0099	2.42	0.0147
$X_2$	1.2012	0.0209	0.55	0.0486	0.25312	0.0015	0.6612	0.04396	3.511	0.0368
$X_3$	30 640.50	0.0401	50.00	<0.0001	0.20225	<0.0391	278.48	<0.0001	1125.8	<0.0001
$X_1X_2$	34 114.09	<0.0001	0.09	0.3921	0.0227	<0.0001	51.1225	0.0087	83.72	<0.0001
$X_1X_3$	213.16	0.0016	3.42	0.0008	0.797	0.3719	70.56	0.0003	18.923	0.0024
$X_2X_3$	3243.30	<0.0001	7.02	<0.0001	0.1225	<0.0001	114.49	<0.0001	3.24	0.0969
$X_1^2$	2692.45	<0.0001	0.17	0.2523	0.0028	<0.0571	1.580	0.3521	7.1158	0.0251
$X_2^2$	28 527.78	<0.0001	1.05	0.0169	0.012	<0.0081	2.29013	0.2692	0.06579	0.7927
$X_3^2$	9226.99	<0.0001	193.27	<0.0001	0.0905	<0.0001	1745.82	<0.0001	1285.79	<0.0001
Residual	60.75		0.96		0.925		11.1325		9.7648	
Lack of fit	57.55	0.671	0.72	0.384	0.692	0.472	8.063	0.0781	6.0275	0.582
Pure error	3.20		0.24		0.233		3.06		3.737	
$R^2$	0.9988		0.9271		0.9570		0.9227		0.9644	
Adjusted $R^2$	0.9943		0.8632		0.8765		0.8972		0.9056	
CV	0.87		1.20		1.0863		1.51		1.135	
PRESS	925.84		12.12		11.08		178.12		98.840	
Adequacy precision	109.36		44.04		192.604		38.03		51.180	

( $Y_1$ : nm), zeta potential ( $Y_2$ : mV), PDI ( $Y_3$ ) and the antifungal activity against *L. theobromae* ( $Y_4$ : %) and *R. stolonifer* ( $Y_5$ : %) were examined through response surface methodology using BBD. The response data for the process variables at each level (-1, 0, +1) had a total of 17 experimental runs and were summarized (Table 2).

The experimental data of particle size ( $Y_1$ ) were fitted to the regression equation and the predicted second-order polynomial mathematical models were expressed in terms of coded values as follows:

$$\text{Particle size} = 265.50 + 31.20X_1 - 0.39X_2 + 61.89X_3 + 92.35X_1X_2 + 7.30X_1X_3 - 28.47X_2X_3 + 25.29X_1^2 + 82.31X_2^2 + 46.81X_3^2$$

Here,  $X_1$ ,  $X_2$  and  $X_3$  are the CH, GA and DP concentrations, respectively. The ANOVA (Table 3) for the particle size showed that the  $R^2$  values were about 0.9988. Generally, the  $R^2$  values determine the goodness of the model, and a higher value indicates a better model.<sup>32</sup> In addition, the *p*-values of particle size for linear, quadratic and interaction terms were significant ( $p < 0.05$ ). The lack of fit value suggests that the model fitted well with the experimental data.

The experimental data of zeta potential ( $Y_2$ ) were fitted to the regression equation, and the predicted second-order polynomial mathematical models were expressed in terms of coded values as follows.

$$\text{Zeta potential} = 24.48 + 0.56X_1 + 0.26X_2 - 2.50X_3 - 0.15X_1X_2 + 0.92X_1X_3 + 1.32X_2X_3 + 0.20X_1^2 - 0.50X_2^2 + 6.78X_3^2$$

Here,  $X_1$ ,  $X_2$  and  $X_3$  are the CH, GA and DP concentrations, respectively. The ANOVA (Table 3) for the zeta potential showed that the  $R^2$  values were about 0.9271, which indicates a better model. The *p*-values of zeta potential for linear, quadratic (except  $X_1^2$ ) and interaction (except  $X_1X_2$ ) terms were significant ( $p < 0.05$ ). The lack of fit value suggests that the model fitted well with the experimental data.

The experimental data of PDI ( $Y_3$ ) were fitted to the regression equation, and the predicted second-order polynomial mathematical models were expressed in terms of coded values as follows:

$$\text{PDI} = 0.18 + 0.071X_1 + 0.005X_2 + 0.16X_3 + 0.075X_1X_2 + 0.005X_1X_3 - 0.018X_2X_3 + 0.023X_1^2 + 0.054X_2^2 + 0.15X_3^2$$

Here,  $X_1$ ,  $X_2$  and  $X_3$  are the CH, GA and DP concentrations, respectively. The ANOVA (Table 3) for the PDI showed that the  $R^2$  values were about 0.9570, which indicates a better model. The *p*-values of the PDI for linear, quadratic and interaction terms (except  $X_1X_3$ ) were significant ( $p < 0.05$ ). The lack of fit value suggests that the model fitted well with the experimental data.

The experimental data of antifungal activity against *L. theobromae* ( $Y_4$ ) and *R. stolonifer* ( $Y_5$ ) were fitted to the regression equation, and the predicted second-order polynomial mathematical models were expressed in terms of coded values as follows:

$$\begin{aligned} \text{Antifungal activity against } L. \text{ theobromae} \\ = 93.20 - 1.56X_1 - 0.29X_2 + 5.90X_3 - 3.57X_1X_2 - 4.20X_1X_3 \\ - 5.35X_2X_3 + 0.61X_1^2 - 0.74X_2^2 - 20.36X_3^2 \end{aligned}$$



Antifungal activity against *R. stolonifer*

$$= 90.30 + 0.55X_1 + 0.66X_2 + 11.86X_3 - 4.58X_1X_2 - 2.18X_1X_3 + 0.90X_2X_3 + 1.30X_1^2 + 0.13X_2^2 - 17.48X_3^2$$

Here,  $X_1$ ,  $X_2$  and  $X_3$  are the CH, GA and DP concentrations, respectively. The ANOVA (Table 3) for the antifungal activity against *L. theobromae* and *R. stolonifer* showed that the  $R^2$  values were about 0.9227 and 0.9644, respectively, indicating a better model. The  $p$ -values of antifungal activity against *L. theobromae* for linear, quadratic (except  $X_1^2$  and  $X_3^2$ ), and interaction terms were significant ( $p < 0.05$ ). The  $p$ -values of antifungal activity against *R. stolonifer* for linear, quadratic (except  $X_2^2$ ), and interaction (except  $X_2X_3$ ) terms were significant ( $p < 0.05$ ). The lack of fit value suggests that the model fitted well with the experimental data.

### Influence of process variables on particle size of the coating solution

The generation of a stable CC-NE system involves the formation of small droplet sizes that are resistant to particle aggregation, enhancing the bioavailability of the bioactive components from LGEO. The effect of the independent variable on the particle

size was presented as a statistical outcome (Table 3). Fig. 1 depicts the response surface plots of the effects of two independent factors on the particle size. Here, when analysing the interaction of two independent variables, the third factor was set to level zero. Fig. 1 also suggests that the particle size of the CC-NE was reduced at low levels of CH concentration, moderate levels of GA concentration and low levels of DP concentration. The effect could be explained by the fact that interfacial tension between the oil and the aqueous phase was reduced, wherein the CH provided a successful coating over the nanodroplets and GA helped in stabilizing the formed NE.<sup>30</sup> Fig. 1A depicts that an increase in the particle size of the CC-NE was observed with the increase in the percentage concentration of CH. The particle size decreases with the increasing concentration of GA and reaches the lowest value at a concentration of 2%, after which the particle size increases gradually. The results reveal that the high CH and low GA concentrations caused larger and more aggregate particles, and a similar result was observed when an oil-in-water emulsion was stabilized by CH and GA complexes.<sup>21</sup> Additionally, Fig. 1B shows that the particle size was comparatively increased when the DP concentration and CH concentration were increased, contrary to the addition of GA beyond

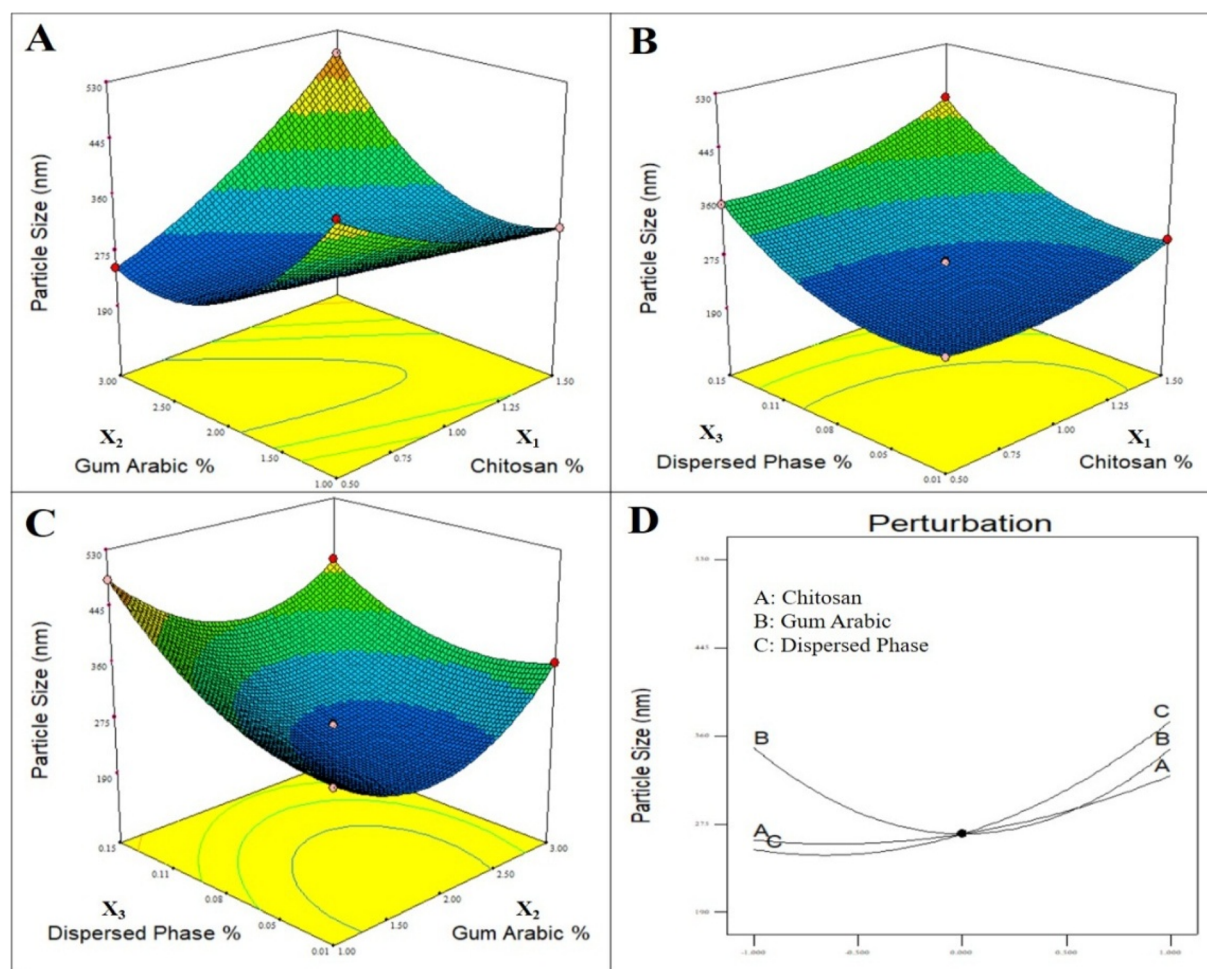


Fig. 1 Influence of process variables on the particle size (nm) of chitosan coated nanoemulsion solution, (A)  $X_1X_2$ ; (B)  $X_1X_3$ ; (C)  $X_2X_3$  interactions; (D) perturbation graph.



2%. A large increase in the particle size at higher CH levels suggests the occurrence of a high amount of non-adsorbed polymers.<sup>47</sup> Fig. 1C indicates that smaller nanosized particles were produced at an increasing concentration of GA and decreasing concentration of DP, indicating the stability of the encapsulated NE. The stabilizer added to the NE acts rapidly and gets adsorbed onto the droplet surface, wherein increasing the GA concentration leads to further reduction of particle size. Here, GA was used to inhibit droplet growth, and several other studies used lecithin as an Ostwald ripening inhibitor.<sup>48</sup> The perturbation plots revealed the comparative effects of all process parameters on the particle size (Fig. 1D). The graphs suggest that the concentration of CH, GA and DP is essential in determining the optimum particle size of CC-NEs. A smaller particle size resulted in greater efficiency of the NE, thus preventing the separation of the two immiscible phases. Research by Fachel *et al.* (2018)<sup>49</sup> has shown the stability of the NE with the addition of CH. Similarly, Yakoubi *et al.* (2021)<sup>50</sup> also created

a phase-stable NE with EOs by optimizing the process parameters. Likewise, Astutiningsih *et al.* (2022)<sup>51</sup> also reported similar effects on particle size by incorporating a CH and GA complex on a saffron essential oil-based nanoemulsion.

### Influence of process variables on zeta potential of the coating solution

The electric potential of the colloidal dispersion was determined using the zeta potential values. The zeta potential values are essential to evaluate the stability of the CC-NE, as ensuring the stability of the NE offers enhanced availability and controlled release of bioactive components from lemongrass essential oil. A positive charge of the zeta potential indicates the net electric charge of the particles in a dispersion. The effect of the independent variable on the zeta potential was presented as a statistical outcome (Table 3). Fig. 2 depicts the response surface plots of the effects of two independent factors on the

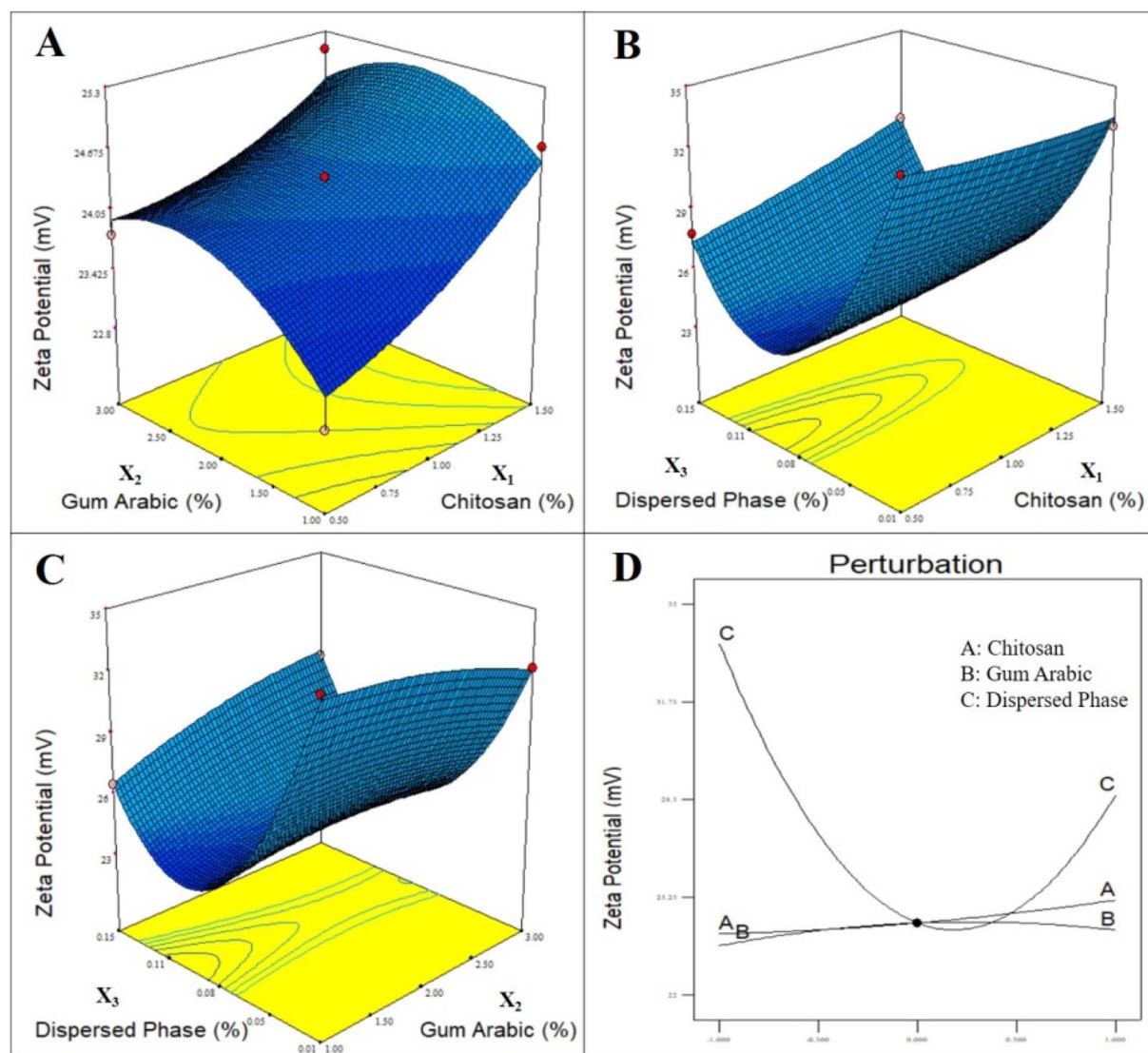


Fig. 2 Influence of process variables on the zeta potential (mV) of chitosan coated nanoemulsion solution, (A)  $X_1X_2$ ; (B)  $X_1X_3$ ; (C)  $X_2X_3$  interactions; (D) perturbation graph.



surface charge of the coating solution. Fig. 2A suggests that an increase in GA (1–2%) and CH (0.5–1.5%) concentrations leads to an increase in the zeta potential values. The positive charges of CH promote the electrostatic interaction with the GA complexes and enhance the stability of the system. The effect can contribute to the increased repulsive forces between the particles, thus resulting in an increase in zeta potential values with the increase in the concentration of the CH/GA complex. In general, zeta potential values in the range of  $-30$  mV to  $30$  mV suggest the stability of the formulations.<sup>49</sup> The zeta potential values of all the runs were in the range of  $22$  to  $34$  mV, and similar results were obtained for a thyme oil incorporating NE coated with CH and whey protein isolate.<sup>47</sup> A high absolute value of zeta potential indicates enhanced stability to coalescence or aggregation. Fig. 2B and C show that the zeta potential values decrease with the increase in the concentration of the DP. The GA and CH molecules adsorb onto the oil–water

interphase, and any changes in the concentration of the DP may lead to alterations in the interface interactions, causing the variations. Moreover, the presence of Tween 80 surfactants and their interaction with the LGEO may result in different charges or surface activity, affecting the overall zeta potential values. The results are supported by clove EO-based NE coating solutions containing sodium alginate, where a decrease in zeta potential values was observed with the addition of the NE.<sup>52</sup> The perturbation plots revealed the comparative effects of all process parameters on the zeta potential (Fig. 2D). The sharp curvature in CH, GA and DP concentrations showed that there was a lower effect of DP content on the zeta potential values, as compared to CH and GA contents. When the concentration of DP increases, the solution is less stable and tends to aggregate; thus, the attractive forces between the molecules are stronger than the repulsive forces.<sup>51</sup> However, the CH content in the coating solution played an important role in surface charge,

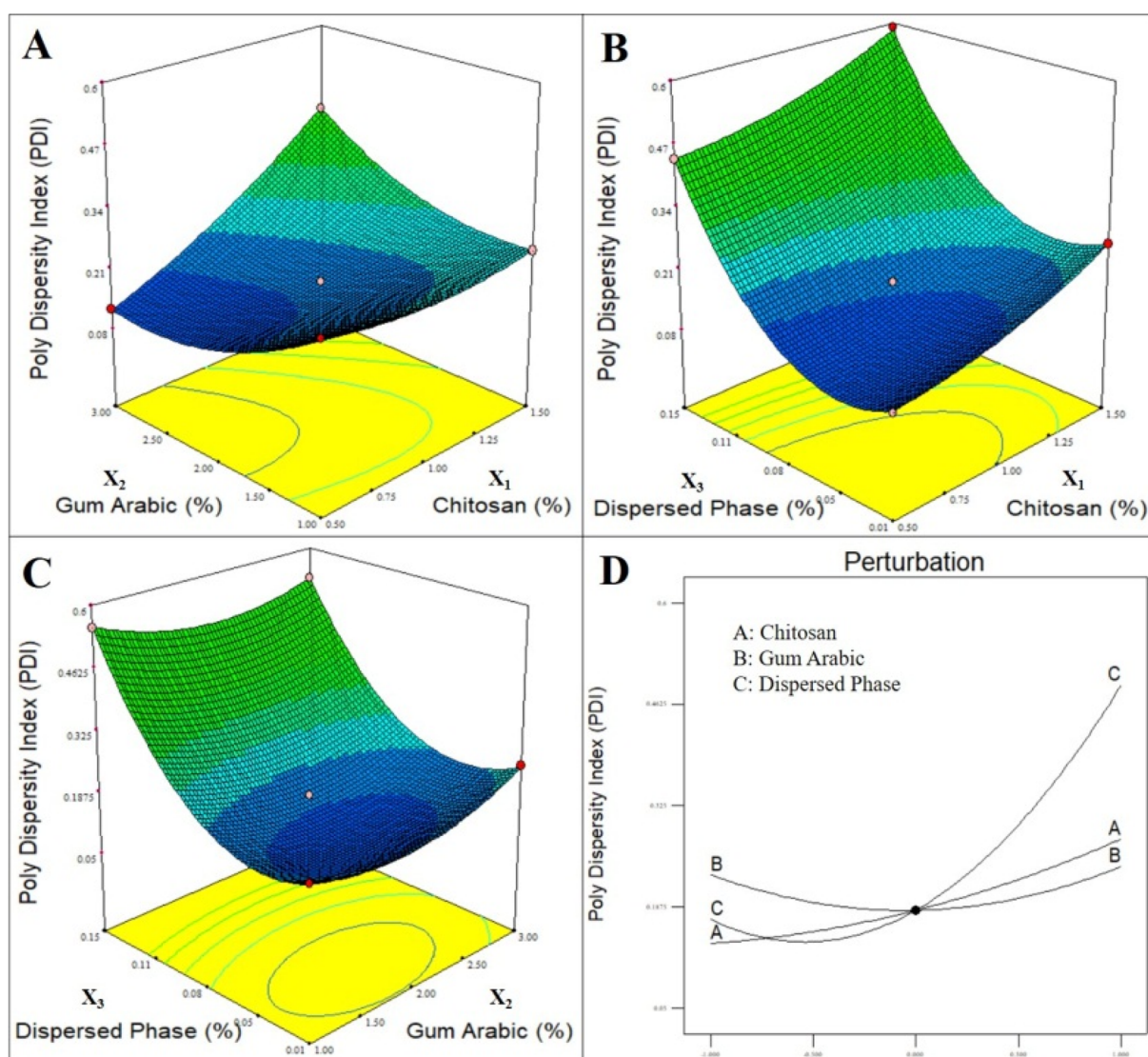


Fig. 3 Influence of process variables on the polydispersity index of chitosan coated nanoemulsion solution, (A)  $X_1X_2$ ; (B)  $X_1X_3$ ; (C)  $X_2X_3$  interactions; (D) perturbation graph.



which increases with an increase in the concentration of the CC-NE. Few studies<sup>37,53</sup> also reported negative zeta potential values, which may arise from the negatively charged functional groups on the particle surface. Regardless of whether the charge is positive or negative, a significant zeta potential value ensures the stability of the solutions by hindering particle aggregations.

### Influence of process variables on the PDI of the coating solution

PDI is a dimensionless parameter used to quantify the homogeneity or heterogeneity in the size distribution of the particles present in the colloidal suspension system.<sup>54</sup> The values close to zero indicate that the coating solutions contain a monodisperse system with a narrow particle size distribution.<sup>47</sup> The homogeneous particle systems allow for an effective encapsulation of EO and enhance the adsorption of the coating material. The effect of the independent variable on the PDI was presented as

a statistical outcome (Table 3). Fig. 3 depicts the response surface plots of the effects of two independent factors on the PDI of the coating solution. Fig. 3A shows that the PDI increases with an increase in the concentration of CH (0.5–1.5%). In contrast, the PDI values decreased with an increase in the GA concentration (1–2%). Then the PDI values increased with an increase in GA beyond 2% concentration. The higher concentration of CH and GA disturbs the steric and electrostatic stabilization, which may lead to ineffective stabilization of the NE, promoting a broader particle size distribution. The broader nanoparticles in the solution tend to aggregate with one another.<sup>51</sup> Likewise, Fig. 3B shows that an increase in the concentration of DP and CH also increases the PDI values. The higher lipid ratio favoured the formation of larger globular sizes with a wide particle distribution. Similarly, high concentrations of CH limited the breakdown of lipid droplets during the emulsification process. A coinciding result was obtained when

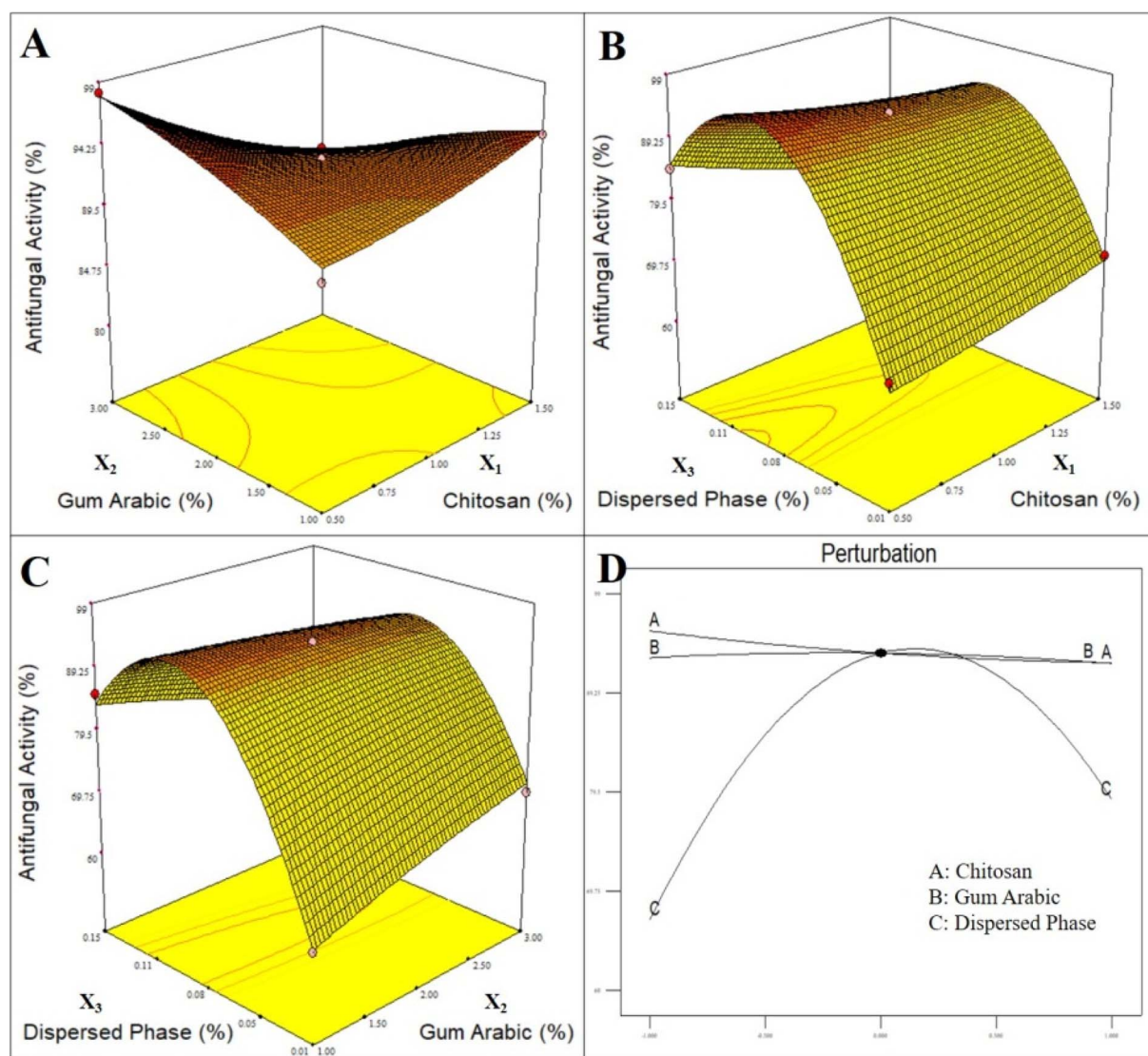


Fig. 4 Influence of process variables on the antifungal activity of chitosan coated nanoemulsion solution against *L. theobromae*, (A)  $X_1X_2$ ; (B)  $X_1X_3$ ; (C)  $X_2X_3$  interactions; (D) perturbation graph.



CH was coated over the NE of nigella oil.<sup>55</sup> When the CH and GA are used together, they may compete for adsorption, and the balance between them could affect the particle size distribution. The competitive adsorption of CH and GA should be controlled through effective formulation in their respective concentrations in the coating solution. A similar result was observed for NEs coated with CH<sup>49</sup> and naringenin loaded with a CH-coated NE.<sup>30</sup> The perturbation plots revealed the comparative effects of all process parameters on the PDI (Fig. 3D). The sharp curvature in GA and DP concentrations showed that there was a lower effect of DP content (0.01–0.08%) on the PDI values, as compared to CH and GA concentrations. However, the GA concentration in the coating solution played an important role in the PDI, and the value decreases with an increase in the concentration up to 2%. Coatings containing CH and GA complexes incorporated with EO-based NEs also produced similar results.<sup>51</sup>

### Influence of process variables on the antifungal activity of coating solution

The antifungal activity of CC-NE solution against *L. theobromae* and *R. stolonifer* was measured in terms of their percentage inhibition on radial mycelial growth. The CC-NE system provides a targeted delivery in inhibiting the growth of *L. theobromae* and *R. stolonifer*. The antifungal activity of the coating solution is a crucial phenomenon that ensures the efficacy of CC-NE in combating the various fungal infections. The effect of the independent variable on the antifungal activity was presented as a statistical outcome (Table 3). Fig. 4 and 5 depict the response surface plots of the effects of two independent factors on the antifungal activity of the coating solution. Fig. 4A and 5A show that antifungal activity against *L. theobromae* and *R. stolonifer* increases with an increase in the concentration of CH

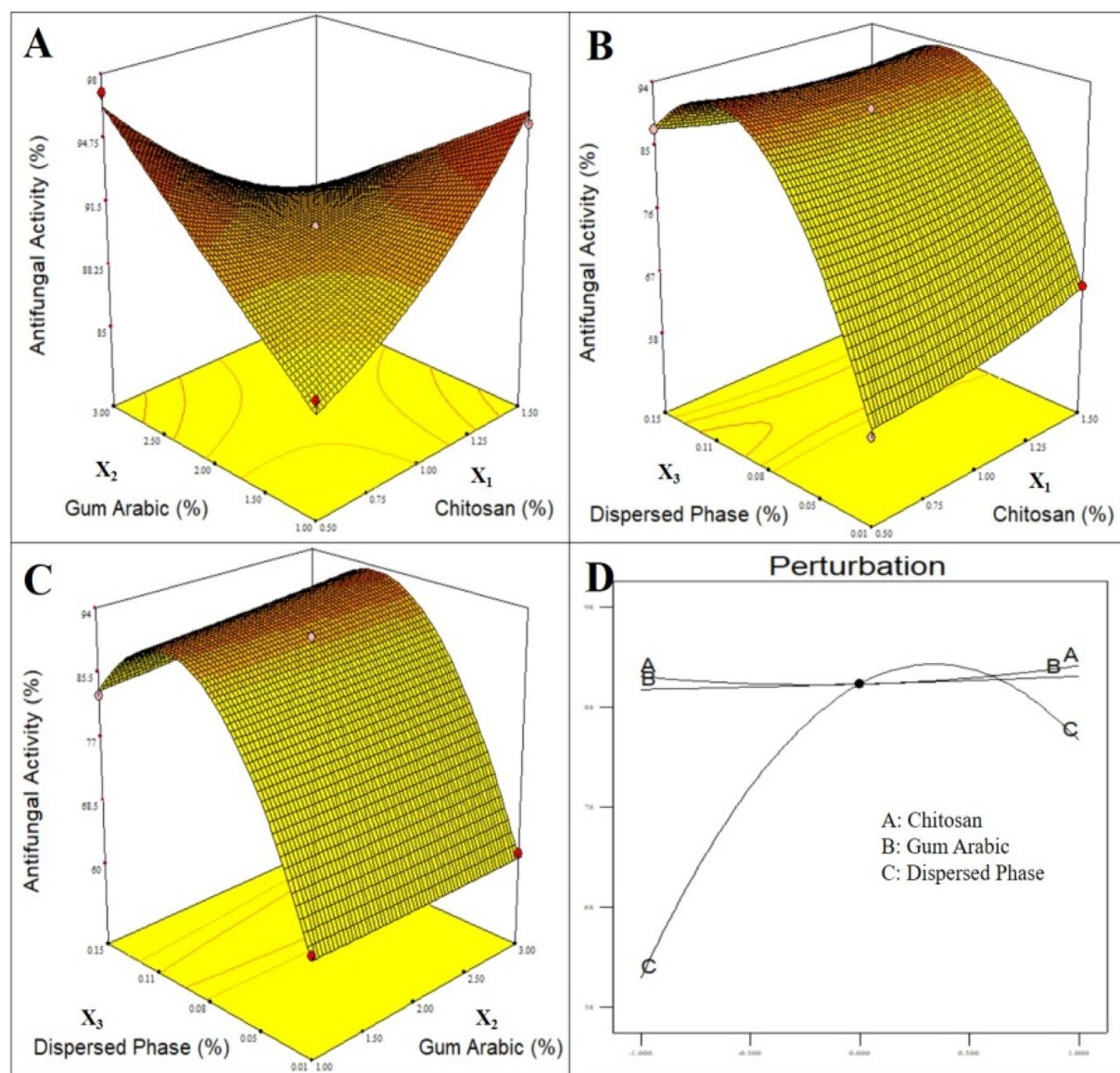


Fig. 5 Influence of process variables on the antifungal activity of chitosan coated nanoemulsion solution against *R. stolonifer*, (A)  $X_1X_2$ ; (B)  $X_1X_3$ ; (C)  $X_2X_3$  interactions; (D) perturbation graph.



and GA. These results are supported by the fact that CH possesses an inherent antimicrobial activity that results in the enhanced inhibition of *L. theobromae* and *R. stolonifer*, respectively. However, the effect of GA on the antifungal activity is not significant. The positively charged CH molecules interact with the negatively charged microbial cell membrane, providing an antifungal effect.<sup>56</sup> Fig. 4B and 5B depict that, with an increase in the concentration of the DP and CH, the antifungal activity of the coating solution against *L. theobromae* and *R. stolonifer* increases. The bioactive components in the DP contribute mainly to the enhanced antifungal properties; hence, the antifungal activity increases with the increase in the DP concentration.<sup>50</sup> The CH in the coating solution forms a protective layer around the droplets, preventing aggregation and aiding in the controlled release of antimicrobial components.<sup>57</sup> Similar to CH and DP interaction, an indistinguishable interaction effect was obtained for GA and DP factors on the antifungal activity against *L. theobromae* and *R. stolonifer* (Fig. 4C and 5C). The addition of GA prevented coalescence and ensured stability, thereby creating a prolonged contact between the NE and the fungal membranes.<sup>58</sup> Moreover, the major bioactive components in the LGEO, geraniol and nerol, are capable of inhibiting the growth of microorganisms.<sup>12</sup> The perturbation plots revealed the comparative effects of all process parameters on the antifungal activity (Fig. 4D and 5D). The DP had the maximum effect in influencing the antifungal activity of both *L. theobromae* and *R. stolonifer*. The synergistic effect of CH and DP was also revealed in the results. A similar result was obtained for coating the papaya fruits with CH and mint EO.<sup>59</sup> Likewise, coatings containing CH and mentha EO prevented the occurrence of postharvest fungal pathogens in papaya fruits.<sup>60</sup>

## Optimization and validation of the model

The optimized model conditions were 0.5% CH, 2.5% GA, and 0.07% DP concentrations with a 0.956 calculated desirability index. The model was verified by performing three replicates under the optimal conditions of the predicted model to validate its predictive capacity. The average values of these three experiments and the predicted values are given in Table 4.

### Characterization of the coating solutions

**Morphology of the coating solutions.** The morphological characteristics of the emulsion at the nanoscale are observed through the TEM technique (Fig. 6). The droplets appear dark and distinct with consistently spherical structures. Here, the coarse emulsion, primary emulsion and CC-NE solution were analysed for morphological studies. The heterogeneity of the coarse emulsion was revealed through broad particle distribution. The primary NE samples reveal droplets without aggregation or clustering, leading to uniformly sized and distributed particles. The GA prevented the coalescence of the oil phase, creating a well-defined, consistent morphology.<sup>51</sup> The CH-NE coating had small-sized droplets with uniform distribution throughout the sample. The visibility of a thin, dark layer around the particles was indicative of the presence of CH covering the droplets, creating a coating over the NE. The layer contributes to the stability and encapsulation of LGEO within the NE. The optimized CC-NE had a smooth surface without any irregularities. The core-shell structure of the LGEO encapsulated within the CH-coated droplets was confirmed through the TEM analysis. A similar structure was obtained for CH coating on curcumin loaded with a NE,<sup>61</sup> a CH-coated NE<sup>55</sup> and a NE incorporated with lemon EO.<sup>62</sup>

**Viscosity of the coating solutions.** The viscosity of coating solutions, coarse emulsion, primary NE and optimized CC-NE was characterized using the viscometer. The colloidal suspension in the small droplet size imparts unique characteristics to the coatings, which could influence the performance of the solution. The viscosity of the coating solutions was considered to be one of the most important parameters in determining the stability of the suspended materials.<sup>35</sup> Generally, NEs exhibit lowered viscosities when compared to traditional emulsion

Table 4 Verification of the model

Responses	Predicted value	Experimental value
Particle size (nm)	229.7	233.5
Zeta potential (mV)	24.52	26.21
PDI	0.110	0.118
Antifungal activity against <i>L. theobromae</i>	95.71	94.78
Antifungal activity against <i>R. stolonifer</i>	91.8	90.62

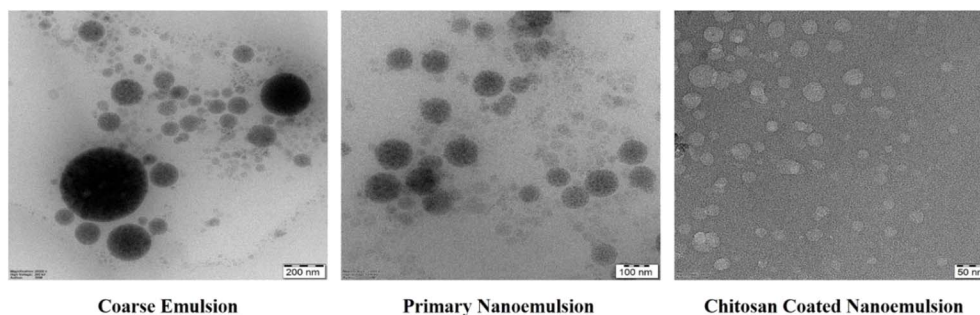


Fig. 6 Morphological characteristics of the nanoemulsion.



Table 5 Characteristic studies of the coating solution<sup>a</sup>

Characterization	Coarse emulsion	Primary nanoemulsion	Chitosan coated nanoemulsion
Viscosity (mPa s)	63.80 ± 0.8 <sup>a</sup>	57.78 ± 0.5 <sup>b</sup>	54.40 ± 0.2 <sup>c</sup>
Turbidity	0.057 ± 0.4 <sup>a</sup>	0.053 ± 0.7 <sup>b</sup>	0.041 ± 0.2 <sup>c</sup>
Whiteness index	40.7 ± 0.3 <sup>a</sup>	43.3 ± 0.6 <sup>b</sup>	45.8 ± 1.0 <sup>c</sup>
Encapsulation efficiency	32.04 ± 0.4 <sup>a</sup>	53.46 ± 0.9 <sup>b</sup>	87.43 ± 0.8 <sup>c</sup>
Loading capacity	0.68 ± 0.5 <sup>a</sup>	1.25 ± 0.7 <sup>b</sup>	3.63 ± 0.6 <sup>c</sup>
Centrifugation stability	68.7 ± 0.3 <sup>a</sup>	37.5 ± 0.5 <sup>b</sup>	No phase separation observed
Heating stability	43.3 ± 0.7 <sup>a</sup>	58.3 ± 0.6 <sup>b</sup>	No phase separation observed
Freezing stability	56.3 ± 0.2 <sup>a</sup>	39.1 ± 0.3 <sup>b</sup>	No phase separation observed

<sup>a</sup> Data were expressed as the mean ± standard deviation of three replicates. The lower-case letters indicate the mean values, with significant differences, according to Duncan's multiple range test ( $p < 0.05$ ).

systems.<sup>54</sup> The reduced droplets in the CC-NE enhance the stability of the solutions by preventing phase separation that occurs over time, and thereby the coating solutions can be stored for a longer period. Table 5 provides the viscosities of the respective coating solutions. Formation of the NE with a balance in the oil phase to aqueous phase ratio, with the appropriate addition of stabilizers and surfactants, controls the droplet sizes of the coating solutions. The viscosities of the coating solutions tend to increase in coarse emulsion and primary NE solutions, which could be attributed to the alterations in the interfacial tension with the addition of significant amounts of surfactants to the solutions. The viscosity of the CC-NE (63.80 ± 0.8 mPa s) was reduced due to the higher surface area per unit volume of the droplets.<sup>30</sup> The lower viscosity levels aid in enhanced flowability, penetration and spreading of coating solutions. Similar results are obtained for NE-based coatings with antimicrobial agents<sup>63</sup> and the CH-coated NE.<sup>49</sup>

**Turbidity of the coating solutions.** Turbidity refers to the degree of opacity or cloudiness of the coating solution. The visual appearance of the coating solutions may be affected by high turbidity levels, leading to increased scattering of light. Here, the coarse emulsion, primary emulsion and CC-NE solution were analysed for turbidity studies. In NE-based coating systems, the turbidity was reduced with the reduction in the droplet diameter. A well-controlled particle size with a narrow distribution was essential in achieving an emulsion with the desired characteristics. Table 5 provides the turbidity values of the respective coating solutions. The turbidity values of the optimized CC-NE solutions are lower when compared with coarse emulsion and primary NE solutions. The clarity and gloss of the coating solutions are affected by the increased turbidity values. The turbidity measurements could be a direct indication of the stability of the coating solutions.<sup>64</sup> The turbidity values change when the particle coagulates and result in phase separation during the storage period. A consistent level of turbidity ensures uniform coverage and well-dispersed coating application. Techniques like ultrasonication and microfluidization also help in retaining the turbidity levels of the coating solution to ensure better coverage.<sup>65</sup> Several studies also suggest similar turbidity values for CH-based NE delivery systems<sup>66</sup> and EO-based microemulsion systems.<sup>36</sup>

### Whiteness index characterization of the coating solutions.

The whiteness index is an important parameter that influences the consumer perception and overall marketability of coating solutions. Achieving appropriate levels of the whiteness index starts with the formulation of the coating solution and process optimization to ensure the functional effectiveness of the coating solution.<sup>36</sup> Consistency in the levels of the whiteness index is essential to meet the market standards of the coating solution; here, the visual identity (bright and appealing) of the solution plays a crucial role. Table 5 provides the whiteness index values of the respective coating solutions. The uniformity of the coating solution in coverage applications was assessed using the whiteness index values and hence could be used as a stability indication tool.<sup>63</sup> The size and distribution of the nanodroplets in the coating solution also influence the whiteness index values.

**Encapsulation efficiency and loading capacity of the coating solutions.** The EE % and LC % of the coating solution are essential in determining the percentage of active components incorporated into the polymeric complexes.<sup>67</sup> This percentage was in direct relation to the antimicrobial efficacy of the coating solutions. A higher encapsulation efficiency indicates a larger portion of EO entrapped within the NE structure. Here, the coarse emulsion, primary emulsion and CC-NE solution were analysed to determine the EE% and LC% (Table 5). The EE (87.43 ± 0.8%) and LC (3.63 ± 0.6%) were higher for the optimized CC-NE coating solution when compared with coarse emulsion and primary NE solutions. The results suggest that the amphiphilic nature of GA enables it to interact with both water and oil, forming a stable emulsion of LGEO. Moreover, GA enhances the compatibility of CH with the oil phase, contributing to the encapsulation of EO and forming a synergistic combination within the system.<sup>68</sup> Additionally, GA also inhibits the occurrence of Oswald ripening in the NE complex, thus contributing to the electrostatic repulsion between the droplets in the emulsion. The CH coating formed around the NE provided a physical barrier to the optimized CC-NE that controls the loaded EO, preventing coalescence and aggregation.<sup>69</sup> Furthermore, the high encapsulation efficiency and loading capacity observed in the CC-NE confirm strong retention of LGEO within the nanoemulsion system. Such efficient encapsulation is critical for minimizing volatilization losses



and enabling sustained release of essential oils during storage. The chitosan interfacial layer further enhances retention through electrostatic interactions and steric stabilization, thereby modulating the release of LGEO. Similar results were obtained for CH-coated NE solution incorporated with wild ginger EO in the prevention of *Aspergillus flavus* (aflatoxin B<sub>1</sub>) contamination.<sup>38</sup>

**Stability studies of the coating solution.** Phase separation or creaming is a process that occurs as the nanoemulsion gets destabilized wherein the oil phase tends to agglomerate into flocs on the top of the system, leaving behind the separated water phase at the bottom.<sup>39</sup> Coating with an unstable emulsion can reduce the effectiveness of its gas and moisture barrier properties, leading to variation in coating thickness and forming a cracked coated surface.<sup>70</sup> Table 5 provides the data for the

stability studies. The CC-NE was found to be the most stable with no flocculation or phase separation as evident from centrifugation, heating and freezing analysis. Here, the NE of the oil phase was stabilized with GA and encapsulated with the CH matrix for controlled release and high-energy ultrasonication created a thermodynamically stable CC-NE solution. A similar result was obtained for a thyme EO-based NE encapsulated with CH for controlling the larvae of mosquito species.<sup>71</sup> Lack of high-energy treatments in the primary NE led to phase separation, wherein the upward movement of oil droplets was observed on centrifugation, heating and freezing processes. The coarse emulsion was neither stabilized with GA nor subjected to ultrasonication, resulting in an emulsion with a high creaming index and prone to spontaneous destabilization on storage. Using ultrasound and homogenization treatments on the

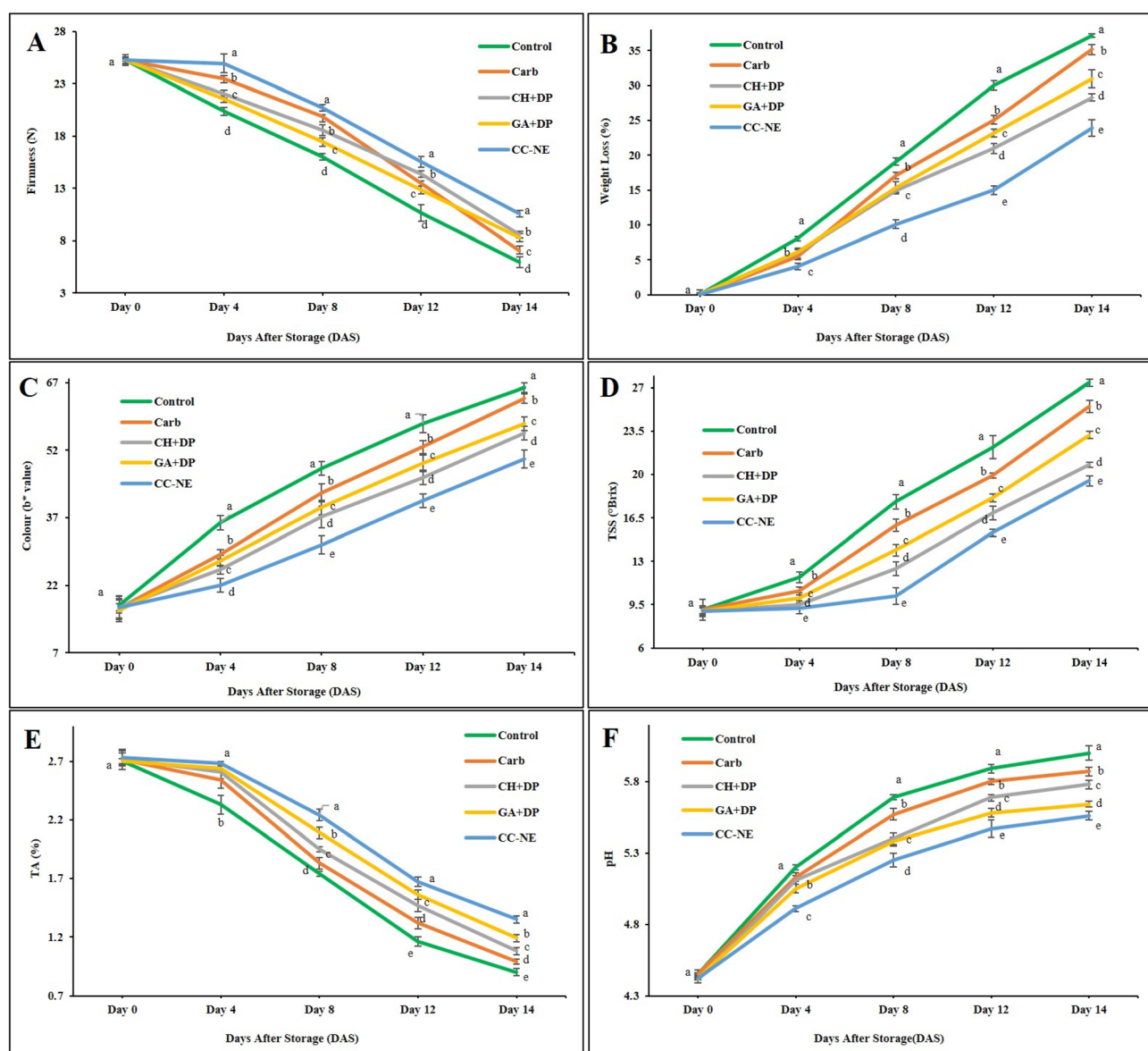


Fig. 7 Effect of the different treatments on the firmness (A), percentage weight loss (B), colour (C), total soluble solids (D), titratable acidity (E) and pH (F) of papaya fruit during the DAS period. Data were expressed as the mean  $\pm$  standard deviation of three replicates. The lower-case letters indicate the mean values, with significant differences, according to Duncan's multiple range test ( $p < 0.05$ ).



emulsion helped produce smaller droplet-sized particles that were stable with no gravitational separation.<sup>39</sup> Likewise, the high-pressure processing of the LGEO-based NE resulted in a stable emulsion with good barrier properties effective for coating fresh berries.<sup>72</sup> The electrostatic repulsion between the smaller and uniform-sized particles is greater, and they are less likely to undergo the destabilization process. The addition of CH aided in regulating the intermolecular forces between the particles, thereby preventing the coalescence of the NE. Several studies prove that CH provides better stability to the emulsion through electrostatic repulsion.<sup>73,74</sup>

### Shelf-life studies on papaya fruits

The shelf-life of papaya fruits in terms of DAS was analysed for all treatment groups. The major determining factor in ensuring the quality of fruits throughout their storage period lies in the controlled firmness values. Fig. 7A reveals that the control groups exhibited higher loss firmness values throughout the storage period, while CC-NE coating significantly ( $p < 0.05$ ) controlled the loss of firmness of papaya fruits (10.58 N) even on the 14th DAS. The decrease in firmness values suggests the possible loss of fruit integrity due to cell wall modifications.<sup>75</sup> This fact might be supported by a universal agreement that climacteric fruits ripen after harvest, and the process of ripening results in the degradation of pectin substances. The damage to the structural tissues of the fruits due to the microbial action also advances the loss of firmness values.<sup>59</sup> In positive control groups, the fruits coated with carbendazim controlled the loss of firmness up to the 8th DAS after which the firmness values decreased rapidly. The result suggests that CC-NE coating could efficiently replace synthetic fungicides by enhancing the shelf-life of fruits up to 14 DAS. Throughout the DAS period, the CC-NE retained the firmness of fruits through a delayed ripening process and controlled postharvest fungal occurrences. Studies suggest that cinnamon EO-based NE coatings exhibited a slow rate of firmness loss to strawberries as the NE provided a physical barrier to water loss and respiration.<sup>34</sup> The terpenes and monoterpene-based bioactive components in the LGEO minimized the substantial loss of firmness due to microbial invasion. Similar results were obtained while coating grape berries with LGEO.<sup>72</sup>

Fig. 7B depicts that the papaya fruits in all treatment groups have a significant ( $p < 0.05$ ) loss in weight percentage through the DAS period. In contrast, the fruits coated with the CC-NE demonstrated the lowest weight loss (23.9%) in the 14 DAS period, whereas the control groups exhibited the highest weight loss of 37.16%. Likewise, a carnauba wax-based NE provided better results in terms of weight loss for papaya fruits.<sup>26</sup> The principle behind the loss of weight in fruits is directly proportional to the water loss from the fruit tissue to the environment.<sup>76</sup> The hydrophobic EO dispersed in the nanosized dimensions in the CH polymeric matrix provides a solid two-dimensional barrier layer to inhibit water and gas evaporation. The stability of the dispersed oil phase in the NE was enhanced with the addition of GA, which provides a viscous liquid or gel sheets between the particles that trap the escaped

gas molecules during respiration. Similar results were obtained for the NE coating of fruits like apples,<sup>76</sup> strawberries<sup>34</sup> and plums.<sup>72</sup> The metabolic reaction and ethylene production also increase the rate of weight loss in fruits.<sup>75</sup> In CC-NE coating, a thick nanometric layer is introduced on the papaya fruit surface that prevents shrivelling and loss of moisture.

The peel colour of fruits is an important parameter as it decides the final fruit quality and consumer acceptability. The process of ripening induces colour changes, which are one of the main factors in judging the maturity of fruits. As the ripening starts, it increases the production of ethylene gases with increased O<sub>2</sub> levels. Fig. 7C depicts that the fruits stored during the DAS period had increased colour values throughout the storage period. The fruits coated with the CC-NE retained the colour values significantly ( $p < 0.05$ ) when compared with the other treatment groups, even in the 14 DAS period. The control and carbendazim-treated fruits revealed a faster change in peel colour. In contrast, the peel colour of the coated fruits changed more slowly, thus minimizing the degradation of chlorophyll and retaining the change in peel colour from green to yellow and orangish red.<sup>77</sup> Similar changes in colour values were observed in grape berries<sup>70</sup> and apples,<sup>63</sup> by coating the surface of the fruits with the LGEO-based NE. The CC-NE with reduced particle size and narrow particle distribution aids in the controlled release of bioactive components of the LGEO, thus restraining the onset of the ripening process and postponing the occurrences of senescence in papaya fruits.

Fig. 7D shows that the TSS values increase significantly ( $p < 0.05$ ) in all treatment groups during the storage period due to the hydrolysis of carbohydrates that results in the formation of simple sugars. An increase in TSS after the harvest period is a natural phenomenon that occurs in climacteric fruits.<sup>75</sup> Generally, active fruit coatings control or minimize the stress that increases the respiration rate. It also prevents the hydrolysis of carbohydrates and reduces the occurrences of fungal growth.<sup>59</sup> The TSS values from the 0th day to the 4th day did not show much difference between the treatment groups. The CC-NE samples from the 4th day to the 8th day of storage retained the TSS values by controlling the hydrolysis of carbohydrate groups. This could possibly be explained as the coating providing a gel barrier to the transfer of gases and slowing down the metabolism that promotes the ripening process. The interactive effects of CH and LGEO in the CC-NE resulted in a denser coating structure with a larger surface area that enhanced the adhesion of the coating material to the layer of papaya, providing moisture/gas barrier properties.<sup>78</sup> The results were consistent with the findings of Oh *et al.* (2017),<sup>70</sup> where LGEO-based NE coatings were used to preserve grape berries and polysaccharide-based NE coatings to improve the storage of apples.<sup>76</sup> The optimized CC-NE coating extended the shelf-life of papaya fruits up to 14 days and successfully retained the physicochemical attributes of papaya.

The TA of the stored papaya fruits tends to decrease over time in all treatment groups due to the utilization of organic acids in the respiration process.<sup>26</sup> As the fruit ripens faster, the organic acids are utilized at a faster rate, leading to a linear decrease in the TA% values. Here, the TA of all coated and



control samples was significantly reduced ( $p < 0.05$ ) at different rates during the DAS period (Fig. 7E). The control samples had a rapid decrease in the TA% values, which is indicative of increased respiration rates compared to the other treatment groups. Similar trends for TA were observed for pectin coatings incorporated with an orange EO-based NE for extending the storage of orange fruits.<sup>78</sup> The results provide clear evidence that the samples coated with the CC-NE had better results when compared with fruits coated with Carb, CH + DP and GA + DP separately. The CC-NE samples showed a slight decrease in the TA % among all groups. This emulsion coating created a deposition on the surface of the fruits, which decreased the gas permeation ability of the fruits. A similar result was reported by Manzoor *et al.* (2021)<sup>79</sup> for coating kiwi fruits with NE-based coatings containing sodium alginate and carboxymethylcellulose. Likewise, papaya fruits coated with  $\alpha$ -limonene-based NE coatings<sup>80</sup> and carnauba wax-based NE coatings<sup>26</sup> also exhibited similar TA % results, wherein the emulsion coatings retained better values.

Fig. 7F depicts the changes in the pH of the coated and uncoated fruits over the DAS period. The observations reveal that the pH of all the treated and control fruits was significantly increased ( $p < 0.05$ ) over the storage time. However, fruits with a moderate rise in pH levels are less prone to rapid ripening and degradation processes. This moderate rise in pH values of the emulsion-coated fruits is due to the decreased consumption of organic acids to be converted to sugars during the ripening process.<sup>25</sup> The prominent increase in the pH of control samples might be because of the proliferation of invasive microorganisms over the storage time, which destabilizes the pH levels.<sup>78</sup> The control fruits exhibit a rapid rise in the pH values when compared with the other treatment groups. The CC-NE coatings resulted in the lowest increase in pH of all treatment groups. A similar result was obtained for NE coatings for strawberries,<sup>81</sup> papaya<sup>26</sup> and oranges.<sup>78</sup> However, for a few fruits like grape

berries<sup>72</sup> and pineapples,<sup>82</sup> insignificant changes in the pH could be observed. The results are possibly attributed to the natural variability of the fruits. In some cases, non-climacteric fruits exhibit insignificant changes as their sugar contents do not change noticeably during the storage period.

### Antifungal activity on the fruit surfaces

The incidence of stem-end rot and fruit rot was significantly lower ( $p < 0.05$ ) in fruits treated with the CC-NE compared to the other treatment groups throughout the storage period. On the 14th day of storage, CC-NE-treated fruits exhibited minimal visible fungal infection, with disease incidence and severity remaining below 10% (Fig. 8). By day 14, the uncoated control and carbendazim-treated fruits showed pronounced fungal growth, surface collapse, and tissue maceration due to senescence and microbial decay. The control fruits, lacking any protective coating, were highly susceptible to microbial colonization, while the fungicide-treated fruits exhibited reduced but still noticeable decay symptoms.<sup>12</sup> In contrast, CC-NE-treated fruits demonstrated superior resistance to fungal infection, which can be attributed to the synergistic antifungal activity of chitosan and sustained release of LCEO. The chitosan coating forms a semi-permeable barrier that restricts oxygen diffusion and microbial penetration,<sup>83</sup> while the nanoemulsion system protects the volatile essential oil from rapid evaporation and thermal degradation.<sup>84</sup> This nanoencapsulation enables controlled release of bioactive compounds, retaining an effective antimicrobial concentration on the fruit surface throughout storage.<sup>85</sup> The enhanced performance of the CC-NE can also be associated with the electrostatic interactions between chitosan and gum arabic, which improve interfacial stability and essential oil retention. Similar controlled-release behaviour and decay inhibition have been reported for essential oil-loaded nanoemulsion coatings applied to tropical fruits.<sup>86,87</sup>

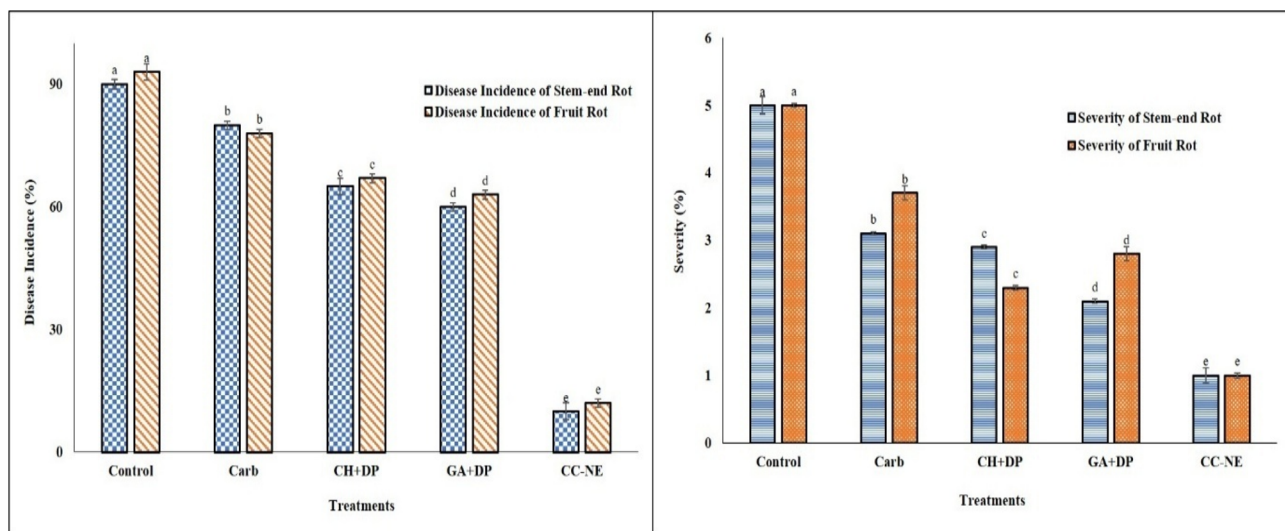


Fig. 8 Effect of the different treatments on the disease incidence and severity of fruit during the 14 DAS period. Data were expressed as the mean  $\pm$  standard deviation of three replicates. The lower-case letters indicate the mean values, with significant differences, according to Duncan's multiple range test ( $p < 0.05$ ).



## Sensory Analysis

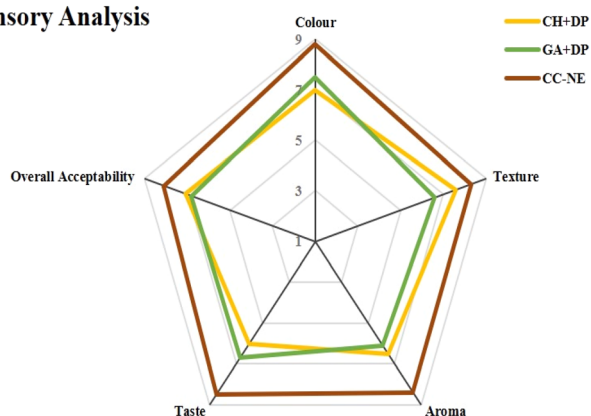


Fig. 9 Effect of different treatments on the sensory parameters of papaya fruits during the 14 DAS period.

## Sensory analysis of the coated papaya fruits

The results of the sensory evaluation of the coated samples on the 14th DAS are presented in Fig. 9. The fruit samples of the CH + DP, GA + DP and CC-NE treatments were analysed based on their colour, texture, aroma, taste and overall acceptance. The parameters had significant differences ( $p < 0.05$ ) between

the various treated fruits on the 14th day of storage. By the 14th day of storage, the control and carbendazim-coated fruits exhibited visible fungal growth, excessive softening, and off-odors rendering them unfit for human consumption; therefore, they were exempted from the sensory analysis. This approach is consistent with previously published postharvest studies,<sup>12</sup> where control fruits that fall below basic edibility thresholds are excluded from sensory panels and discussed qualitatively rather than quantitatively. The sensory scores reveal that the fruits coated with the CC-NE had scored much higher values, and the panelists showed a preference for those fruits. The panelists judged the colour values of the samples based on the fruit's glossiness and uniform ripeness. The CC-NE samples retained better colour scores even after the storage period when compared with CH + DP and GA + DP samples. A similar result was obtained for tomato samples coated with a carnauba wax-based NE.<sup>88</sup> The texture and aroma parameters are considered important as they directly indicate the fruit's freshness. The panelist judged the texture of the fruits based on their firmness and the level of decay occurrence. The incorporation of EO into the coating system predominantly controlled the fungal decay incidence and retained fruit firmness.<sup>82</sup> In CC-NE solutions, the LGEO entrapped in the CH coatings was an added advantage for ensuring the controlled

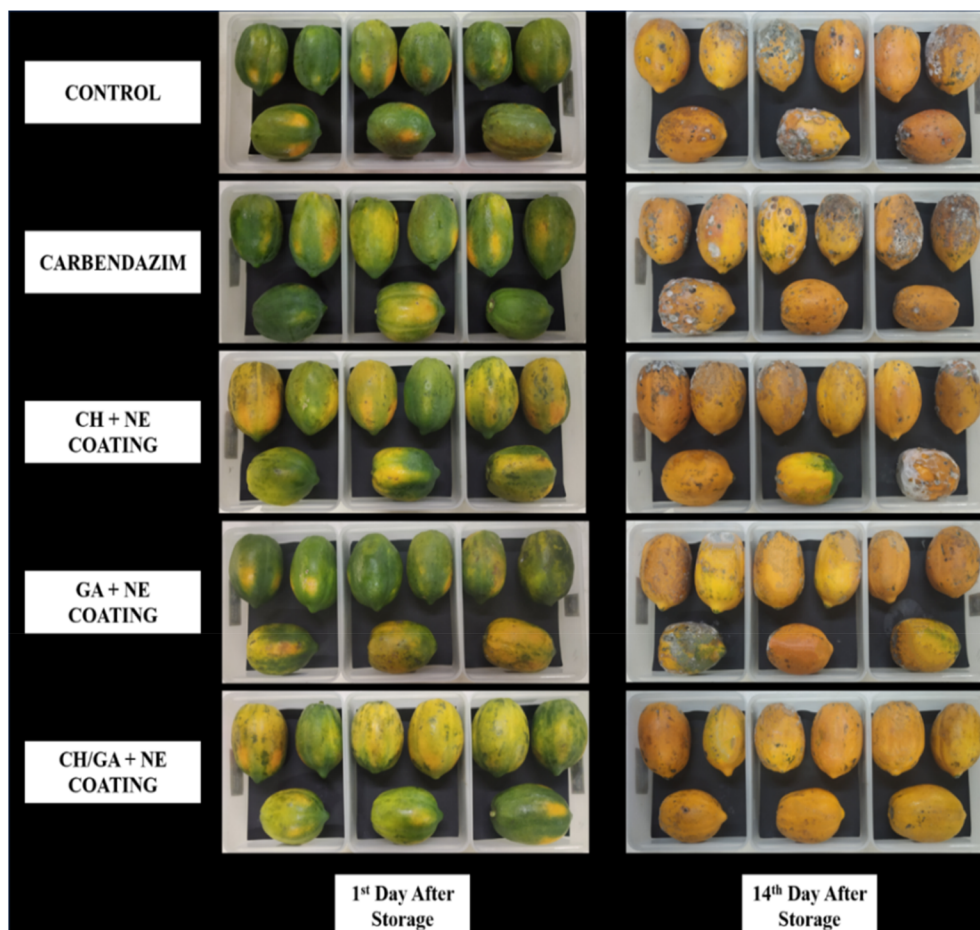


Fig. 10 The stored papaya fruits for shelf-life studies.



release of bioactive components throughout the storage period. There was a significant preference in the aroma scores of the samples coated with the CC-NE. Loading of LGEO in the delivery system increased the aroma sensory scores of the coated samples. The improvement in the aroma of CC-NE samples when compared with CH + DP and GA + DP might be the result of increased volatile compounds of LGEO entrapped in the CH matrix. A study by Chen *et al.* (2022)<sup>66</sup> obtained similar results on coating EO entrapped in CH-based delivery systems for minimally processed produce. A similar result was obtained for papaya fruits coated with a ginger EO-based NE.<sup>24</sup> The highest score for the overall acceptance of the CC-NE suggests that the uniform solubility of LGEO was ensured by adding a good stabilizer like GA. Here, CH was used as an efficient delivery system for coating the dispersed oil phase. Therefore, based on the overall acceptance of the sensory scores, the CC-NE coating may positively influence the consumer's purchase decision. Fig. 10 depicts the photograph of papaya fruits during the storage period.

## Conclusion

This study successfully optimized the process parameters for attaining an effective chitosan-coated nanoemulsion through Box-Behnken design. The concentration of chitosan, gum arabic and dispersed oil phase was identified as the key component in the formulation of an NE. The application of RSM allowed for the identification of optimal formulation parameters, ensuring the most effective CC-NE in terms of particle size, zeta potential, polydispersity index and antifungal activity. The optimized CC-NE exhibited excellent characteristics in terms of morphology, viscosity and turbidity. The encapsulation efficiency was significantly improved for the CC-NE, ensuring the controlled release of bioactive components. The thermodynamic stability studies demonstrated that the fabricated CC-NE solutions remained stable, preventing the occurrence of density separation or degradation. The application of CC-NE on fresh papaya fruits resulted in a significant extension of their shelf-life. Quality indices, including total soluble solids, titratable acidity, and firmness, were better retained in CC-NE treated fruits, indicating that metabolic deterioration was effectively retarded. The superior sensory scores for texture, aroma, and overall acceptability further demonstrated that the formulation not only preserved nutritional attributes but also sustained consumer-relevant qualities. Importantly, the biocompatible and biodegradable nature of chitosan and essential oils ensures food safety, the absence of toxic residues, and environmental sustainability, positioning this technology as a viable alternative to synthetic fungicides. Beyond papaya, the demonstrated approach can be extended to other tropical fruits prone to postharvest decay, potentially reducing economic losses and enhancing supply chain resilience. Future directions should include pilot-scale validation, comprehensive release kinetics modelling, and integration with smart packaging technologies for real-time monitoring of fruit quality. Overall, the papaya fruits coated with the CC-NE exhibited an extended shelf-life of  $14 \pm 1$  days under ambient conditions ( $25 \pm 2$  °C and 70–75%

relative humidity), while preserving their postharvest quality and ensuring a sustainable approach.

## Author contributions

Dharini V.: conceptualization (lead); data curation (lead); investigation (lead); methodology (lead); writing – original draft (lead). Periyar Selvam Sellamuthu: investigation (equal); supervision (supporting); validation (supporting). Jayaramudu J.: validation (supporting). Emmanuel R. Sadiku: visualization (supporting); writing – review and editing (supporting).

## Conflicts of interest

The authors hereby declare that they have no conflict of interest.

## Data availability

Data supporting the findings of this study are available within the article.

## Acknowledgements

We thank the SRM Central Instrumentation Facility (SCIF) and Nanotechnology Research Centre (NRC) of the SRM Institute of Science and Technology for their help and cordial support of our study.

## References

- 1 M. Ali, A. Ali, S. Ali, *et al.*, Global insights and advances in edible coatings or films toward quality maintenance and reduced postharvest losses of fruit and vegetables: An updated review, *Compr. Rev. Food Sci. Food Saf.*, 2025, **24**(1), e70103, DOI: [10.1111/1541-4337.70103](https://doi.org/10.1111/1541-4337.70103).
- 2 R. I. Barbhuiya, C. Wroblewski, S. P. Ravikumar, *et al.*, Enhancing Papaya Shelf-Life with Upcycled Pea Starch-Neem Oil Polymeric Nanoparticles Synthesized via a Novel Rapid Spray Nanoprecipitation Technique, *Polym. Adv. Technol.*, 2025, **36**(8), e70297, DOI: [10.1002/pat.70297](https://doi.org/10.1002/pat.70297).
- 3 F. Liang, J. Geng, Z. Yang, *et al.*, Preparation of amphiphilic chitosan incorporated with ursolic acid active coating films and its delay of postharvest papaya fruit ripening, *Food Packag. Shelf Life*, 2025, **49**, 101514, DOI: [10.1016/j.fpsl.2025.101514](https://doi.org/10.1016/j.fpsl.2025.101514).
- 4 N. N. Chowdhury, M. N. Islam, R. Jafrin, *et al.*, Natural plant products as effective alternatives to synthetic chemicals for postharvest fruit storage management, *Crit. Rev. Food Sci. Nutr.*, 2023, **63**(30), 10332–10350, DOI: [10.1080/10408398.2022.2079112](https://doi.org/10.1080/10408398.2022.2079112).
- 5 M. Iñiguez-Moreno, B. Santiesteban-Romero, E. A. Flores-Contreras, *et al.*, Sustainable Solutions for Postharvest Berry Protection: Natural Edible Coatings, *Food Bioprocess Technol.*, 2024, **17**(11), 3483–3505, DOI: [10.1007/s11947-023-03301-z](https://doi.org/10.1007/s11947-023-03301-z).
- 6 H. C. Moghadas, J. S. Smith and R. Tahergorabi, Recent Advances in the Application of Edible Coatings for Shelf-



- Life Extension of Strawberries: A Review, *Food Bioprocess Technol.*, 2025, **18**(2), 1079–1103, DOI: [10.1007/s11947-024-03517-7](https://doi.org/10.1007/s11947-024-03517-7).
- 7 N. Dayeh, K. Asefpour Vakilian and M. Azadbakht, A fruit edible coating machine to protect the morphological, physiological, and biochemical properties of citrus fruits, *Food Bioprod. Process.*, 2024, **148**, 428–435, DOI: [10.1016/j.fbp.2024.10.017](https://doi.org/10.1016/j.fbp.2024.10.017).
- 8 R. Sharma, P. C. Nath, P. Das, *et al.*, Essential oil-nanoemulsion based edible coating: Innovative sustainable preservation method for fresh/fresh-cut fruits and vegetables, *Food Chem.*, 2024, **460**, 140545, DOI: [10.1016/j.foodchem.2024.140545](https://doi.org/10.1016/j.foodchem.2024.140545).
- 9 S. M. K. Hasan, G. Ferrentino and M. Scampicchio, Nanoemulsion as advanced edible coatings to preserve the quality of fresh-cut fruits and vegetables: a review, *Int. J. Food Sci. Technol.*, 2020, **55**(1), 1–10, DOI: [10.1111/ijfs.14273](https://doi.org/10.1111/ijfs.14273).
- 10 H. Hassanzadeh, S. A. Ahmed and N. S. H. Qadir, Application of the Active Edible Film Reinforced with Nanoparticles and Nanoemulsions as the Coating Systems to Improve the Quality and Shelf Life of Fruits and Vegetables, *J. Nanotechnol.*, 2025, **2025**(1), 7036931, DOI: [10.1155/jnt/7036931](https://doi.org/10.1155/jnt/7036931).
- 11 K. Bajaj, A. Kumar, P. P. S. Gill, S. K. Jawandha, R. Arora and A. Singh, Guar gum and essential oil-based composite coatings preserve antioxidant enzymes activity and postharvest quality of kinnow Mandarin, *Food Biosci.*, 2024, **61**, 104906, DOI: [10.1016/j.fbio.2024.104906](https://doi.org/10.1016/j.fbio.2024.104906).
- 12 V. Dharini, P. S. S, J. J and R. E. Sadiku, Effect of functionalized hybrid chitosan/gum Arabic bilayer coatings with lemongrass essential oil on the postharvest disease control and the physicochemical properties of papaya (*Carica papaya*) fruits, *S. Afr. J. Bot.*, 2023, **160**, 602–612, DOI: [10.1016/j.sajb.2023.07.053](https://doi.org/10.1016/j.sajb.2023.07.053).
- 13 M. F. Almeida, G. L. Silva, G. D. Gondim, *et al.*, Maintenance of postharvest quality of ‘Palmer’ mango coated with biodegradable coatings based on cassava starch and emulsion of lemongrass essential oil, *Int. J. Biol. Macromol.*, 2024, **277**, 134323, DOI: [10.1016/j.ijbiomac.2024.134323](https://doi.org/10.1016/j.ijbiomac.2024.134323).
- 14 X. Wang, Z. Xue, Y. Sun, B. Peng, C. Wu and X. Kou, Chitosan-ginger essential oil nanoemulsions loaded gelatin films: A biodegradable material for food preservation, *Int. J. Biol. Macromol.*, 2024, **280**, 135791, DOI: [10.1016/j.ijbiomac.2024.135791](https://doi.org/10.1016/j.ijbiomac.2024.135791).
- 15 M. Radi, S. Shadikhah, M. Sayadi, S. Kaveh, S. Amiri and F. Bagheri, Effect of Thymus vulgaris Essential Oil-Loaded Nanostructured Lipid Carriers in Alginate-Based Edible Coating on the Postharvest Quality of Tangerine Fruit, *Food Bioprocess Technol.*, 2023, **16**(1), 185–198, DOI: [10.1007/s11947-022-02914-0](https://doi.org/10.1007/s11947-022-02914-0).
- 16 K. Sapna, C. Sharma, P. Pathak and S. Gautam, Chitosan Edible Coatings Loaded with Bioactive Components for Fruits and Vegetables: A Step Toward Sustainable Development Goals, *Food Bioprocess Technol.*, 2025, **18**(6), 4975–5009, DOI: [10.1007/s11947-025-03770-4](https://doi.org/10.1007/s11947-025-03770-4).
- 17 C. Xie, Y. Wang, D. Yang, Y. Zhong and K. Fan, Polysaccharide-Based Edible Film/Coating Incorporated with Nano-Antimicrobial Agent for Improving Quality of Fruits and Vegetables: A Review, *Food Rev. Int.*, 2025, 1–33, DOI: [10.1080/87559129.2025.2524401](https://doi.org/10.1080/87559129.2025.2524401).
- 18 L. T. C. Maswanganye, S. K. Pillai and D. Sivakumar, Chitosan Coating Loaded with Spearmint Essential Oil Nanoemulsion for Antifungal Protection in Soft Citrus (*Citrus reticulata*) Fruits, *Coatings*, 2025, **15**(1), 105, DOI: [10.3390/coatings15010105](https://doi.org/10.3390/coatings15010105).
- 19 S. Dhanasekaran, L. Liang, S. Gurusamy, Q. Yang and H. Zhang, Chitosan stabilized lemon essential oil nanoemulsion controls black mold rot and maintains quality of table grapes, *Int. J. Biol. Macromol.*, 2024, **277**, 134251, DOI: [10.1016/j.ijbiomac.2024.134251](https://doi.org/10.1016/j.ijbiomac.2024.134251).
- 20 B. Muhoza, S. Xia, X. Wang, X. Zhang, Y. Li and S. Zhang, Microencapsulation of essential oils by complex coacervation method: preparation, thermal stability, release properties and applications, *Crit. Rev. Food Sci. Nutr.*, 2022, **62**(5), 1363–1382, DOI: [10.1080/10408398.2020.1843132](https://doi.org/10.1080/10408398.2020.1843132).
- 21 N. Zhang, J. Han, F. Chen, C. Gao and X. Tang, Chitosan/gum arabic complexes to stabilize Pickering emulsions: Relationship between the preparation, structure and oil-water interfacial activity, *Food Hydrocolloids*, 2022, **129**, 107532, DOI: [10.1016/j.foodhyd.2022.107532](https://doi.org/10.1016/j.foodhyd.2022.107532).
- 22 J. Han, F. Chen, C. Gao, Y. Zhang and X. Tang, Environmental stability and curcumin release properties of Pickering emulsion stabilized by chitosan/gum arabic nanoparticles, *Int. J. Biol. Macromol.*, 2020, **157**, 202–211, DOI: [10.1016/j.ijbiomac.2020.04.177](https://doi.org/10.1016/j.ijbiomac.2020.04.177).
- 23 M. C. Yu, C. Y. Hou, J. S. Tsay, H. Y. Chung, P. H. Huang and Y. S. Liang, Evaluating the application feasibility of thyme oil nanoemulsion coating for extending the shelf life of papaya (*Carica papaya* cv. Tainung No. 2) with postharvest physiology and quality parameters, *Chem. Biol. Technol. Agric.*, 2024, **11**(1), 74, DOI: [10.1186/s40538-024-00598-6](https://doi.org/10.1186/s40538-024-00598-6).
- 24 M. Miranda, X. Sun, A. Marin, *et al.*, Nano- and micro-sized carnauba wax emulsions-based coatings incorporated with ginger essential oil and hydroxypropyl methylcellulose on papaya: Preservation of quality and delay of post-harvest fruit decay, *Food Chem.: X*, 2022, **13**, 100249, DOI: [10.1016/j.fochx.2022.100249](https://doi.org/10.1016/j.fochx.2022.100249).
- 25 J. G. D. Oliveira Filho, G. D. C. Silva, F. C. A. Oldoni, *et al.*, Edible Coating Based on Carnauba Wax Nanoemulsion and Cymbopogon martinii Essential Oil on Papaya Postharvest Preservation, *Coatings*, 2022, **12**(11), 1700, DOI: [10.3390/coatings12111700](https://doi.org/10.3390/coatings12111700).
- 26 J. G. D. Oliveira Filho, L. G. R. Duarte, Y. B. B. Silva, *et al.*, Novel Approach for Improving Papaya Fruit Storage with Carnauba Wax Nanoemulsion in Combination with Syzygium aromaticum and Mentha spicata Essential Oils, *Coatings*, 2023, **13**(5), 847, DOI: [10.3390/coatings13050847](https://doi.org/10.3390/coatings13050847).
- 27 C. W. T. Fukuyama, L. G. R. Duarte, I. C. Pedrino, M. C. Mitsuyuki, S. B. Junior and M. D. Ferreira, Effect of carnauba wax nanoemulsion associated with *Syzygium aromaticum* and *Mentha piperita* essential oils as an



- alternative to extend lychee post-harvest shelf life, *Sustainable Food Technol.*, 2024, 2(2), 426–436, DOI: [10.1039/D3FB00251A](https://doi.org/10.1039/D3FB00251A).
- 28 B. Tafa, Y. W. Tariku and R. Duraisamy, Maintaining fruit quality and reducing waste: A pectin-rosemary nano-emulsion coating for apple and banana preservation, *Appl. Food Res.*, 2025, 5(2), 101317, DOI: [10.1016/j.afres.2025.101317](https://doi.org/10.1016/j.afres.2025.101317).
- 29 P. S. U. Putra, D. R. Adhika, G. Genecya, M. S. Al Madanie and L. A. T. W. Asri, Evaluation of Chitosan-Encapsulated Lemongrass (*Cymbopogon citratus*) Essential Oil Nanoemulsion for Fruit Edible Coating, *OpenNano*, 2025, 24, 100246, DOI: [10.1016/j.onano.2025.100246](https://doi.org/10.1016/j.onano.2025.100246).
- 30 S. H. Akrawi, B. Gorain, A. B. Nair, *et al.*, Development and Optimization of Naringenin-Loaded Chitosan-Coated Nanoemulsion for Topical Therapy in Wound Healing, *Pharmaceutics*, 2020, 12(9), 893, DOI: [10.3390/pharmaceutics12090893](https://doi.org/10.3390/pharmaceutics12090893).
- 31 S. B. Murmu and H. N. Mishra, Optimization of the arabic gum based edible coating formulations with sodium caseinate and tulsi extract for guava, *LWT*, 2017, 80, 271–279, DOI: [10.1016/j.lwt.2017.02.018](https://doi.org/10.1016/j.lwt.2017.02.018).
- 32 S. Hajji, I. Younes, S. Affes, S. Boufi and M. Nasri, Optimization of the formulation of chitosan edible coatings supplemented with carotenoproteins and their use for extending strawberries postharvest life, *Food Hydrocolloids*, 2018, 83, 375–392, DOI: [10.1016/j.foodhyd.2018.05.013](https://doi.org/10.1016/j.foodhyd.2018.05.013).
- 33 G. Khaliq, M. M. T. Muda, A. Ali, P. Ding and H. M. Ghazali, Effect of gum arabic coating combined with calcium chloride on physico-chemical and qualitative properties of mango (*Mangifera indica* L.) fruit during low temperature storage, *Sci. Hortic.*, 2015, 190, 187–194, DOI: [10.1016/j.scienta.2015.04.020](https://doi.org/10.1016/j.scienta.2015.04.020).
- 34 Y. Chu, C. Gao, X. Liu, *et al.*, Improvement of storage quality of strawberries by pullulan coatings incorporated with cinnamon essential oil nanoemulsion, *LWT*, 2020, 122, 109054, DOI: [10.1016/j.lwt.2020.109054](https://doi.org/10.1016/j.lwt.2020.109054).
- 35 S. M. T. Gharibzahedi, Ultrasound-mediated nettle oil nanoemulsions stabilized by purified jujube polysaccharide: Process optimization, microbial evaluation and physicochemical storage stability, *J. Mol. Liq.*, 2017, 234, 240–248, DOI: [10.1016/j.molliq.2017.03.094](https://doi.org/10.1016/j.molliq.2017.03.094).
- 36 S. Basak and P. Guha, Betel leaf (*Piper betle* L.) essential oil microemulsion: Characterization and antifungal activity on growth, and apparent lag time of *Aspergillus flavus* in tomato paste, *LWT*, 2017, 75, 616–623, DOI: [10.1016/j.lwt.2016.10.021](https://doi.org/10.1016/j.lwt.2016.10.021).
- 37 Ö. Tastan, G. Ferrari, T. Baysal and F. Donsi, Understanding the effect of formulation on functionality of modified chitosan films containing carvacrol nanoemulsions, *Food Hydrocolloids*, 2016, 61, 756–771, DOI: [10.1016/j.foodhyd.2016.06.036](https://doi.org/10.1016/j.foodhyd.2016.06.036).
- 38 Deepika, A. Singh, A. K. Chaudhari, S. Das and N. K. Dubey, Zingiber zerumbet L. essential oil-based chitosan nanoemulsion as an efficient green preservative against fungi and aflatoxin B<sub>1</sub> contamination, *J. Food Sci.*, 2021, 86(1), 149–160, DOI: [10.1111/1750-3841.15545](https://doi.org/10.1111/1750-3841.15545).
- 39 A. R. Locali-Pereira, J. S. Guazi, A. C. Conti-Silva and V. R. Nicoletti, Active packaging for postharvest storage of cherry tomatoes: Different strategies for application of microencapsulated essential oil, *Food Packag. Shelf Life*, 2021, 29, 100723, DOI: [10.1016/j.fpsl.2021.100723](https://doi.org/10.1016/j.fpsl.2021.100723).
- 40 M. H. Lee, S. Y. Kim and H. J. Park, Effect of halloysite nanoclay on the physical, mechanical, and antioxidant properties of chitosan films incorporated with clove essential oil, *Food Hydrocolloids*, 2018, 84, 58–67, DOI: [10.1016/j.foodhyd.2018.05.048](https://doi.org/10.1016/j.foodhyd.2018.05.048).
- 41 G. Khaliq, M. Ramzan and A. H. Baloch, Effect of Aloe vera gel coating enriched with *Fagonia indica* plant extract on physicochemical and antioxidant activity of sapodilla fruit during postharvest storage, *Food Chem.*, 2019, 286, 346–353, DOI: [10.1016/j.foodchem.2019.01.135](https://doi.org/10.1016/j.foodchem.2019.01.135).
- 42 P. Kumar, S. Sethi, R. R. Sharma, M. Srivastav and E. Varghese, Effect of chitosan coating on postharvest life and quality of plum during storage at low temperature, *Sci. Hortic.*, 2017, 226, 104–109, DOI: [10.1016/j.scienta.2017.08.037](https://doi.org/10.1016/j.scienta.2017.08.037).
- 43 L. L. Daisy, J. M. Nduko, W. M. Joseph and S. M. Richard, Effect of edible gum Arabic coating on the shelf life and quality of mangoes (*Mangifera indica*) during storage, *J. Food Sci. Technol.*, 2020, 57(1), 79–85, DOI: [10.1007/s13197-019-04032-w](https://doi.org/10.1007/s13197-019-04032-w).
- 44 A. Naem, T. Abbas, T. M. Ali and A. Hasnain, Effect of guar gum coatings containing essential oils on shelf life and nutritional quality of green-unripe mangoes during low temperature storage, *Int. J. Biol. Macromol.*, 2018, 113, 403–410, DOI: [10.1016/j.ijbiomac.2018.01.224](https://doi.org/10.1016/j.ijbiomac.2018.01.224).
- 45 P. S. Sellamuthu, M. Mafune, D. Sivakumar and P. Soundy, Thyme oil vapour and modified atmosphere packaging reduce anthracnose incidence and maintain fruit quality in avocado: Thyme oil vapour and modified atmosphere packaging in avocado, *J. Sci. Food Agric.*, 2013, 93(12), 3024–3031, DOI: [10.1002/jsfa.6135](https://doi.org/10.1002/jsfa.6135).
- 46 P. S. Sellamuthu, D. Sivakumar and P. Soundy, Antifungal Activity and Chemical Composition of Thyme, Peppermint and Citronella Oils in Vapor Phase against Avocado and Peach Postharvest Pathogens, *J. Food Saf.*, 2013, 33(1), 86–93, DOI: [10.1111/jfs.12026](https://doi.org/10.1111/jfs.12026).
- 47 S. Li, J. Sun, J. Yan, *et al.*, Development of antibacterial nanoemulsions incorporating thyme oil: Layer-by-layer self-assembly of whey protein isolate and chitosan hydrochloride, *Food Chem.*, 2021, 339, 128016, DOI: [10.1016/j.foodchem.2020.128016](https://doi.org/10.1016/j.foodchem.2020.128016).
- 48 K. Keykhosravy, S. Khanzadi, M. Hashemi and M. Azizzadeh, Chitosan-loaded nanoemulsion containing Zataria Multiflora Boiss and Bunium persicum Boiss essential oils as edible coatings: Its impact on microbial quality of turkey meat and fate of inoculated pathogens, *Int. J. Biol. Macromol.*, 2020, 150, 904–913, DOI: [10.1016/j.ijbiomac.2020.02.092](https://doi.org/10.1016/j.ijbiomac.2020.02.092).
- 49 F. N. S. Fachel, B. Medeiros-Neves, M. Dal Prá, *et al.*, Box-Behnken design optimization of mucoadhesive chitosan-



- coated nanoemulsions for rosmarinic acid nasal delivery— In vitro studies, *Carbohydr. Polym.*, 2018, **199**, 572–582, DOI: [10.1016/j.carbpol.2018.07.054](https://doi.org/10.1016/j.carbpol.2018.07.054).
- 50 S. Yakoubi, I. Kobayashi, K. Uemura, *et al.*, Essential-Oil-Loaded Nanoemulsion Lipidic-Phase Optimization and Modeling by Response Surface Methodology (RSM): Enhancement of Their Antimicrobial Potential and Bioavailability in Nanoscale Food Delivery System, *Foods*, 2021, **10**(12), 3149, DOI: [10.3390/foods10123149](https://doi.org/10.3390/foods10123149).
- 51 F. Astutiningsih, S. Anggrahini, A. Fitriani and S. Supriyadi, Optimization of Saffron Essential Oil Nanoparticles Using Chitosan-Arabic Gum Complex Nanocarrier with Ionic Gelation Method, *Int. J. Food Sci.*, 2022, **2022**, 1–14, DOI: [10.1155/2022/4035033](https://doi.org/10.1155/2022/4035033).
- 52 V. K. Pandey, S. Srivastava, R. Singh, A. H. Dar and K. K. Dash, Effects of clove essential oil (*Caryophyllus aromaticus* L.) nanoemulsion incorporated edible coating on shelf-life of fresh cut apple pieces, *J. Agric. Food Res.*, 2023, **14**, 100791, DOI: [10.1016/j.jafr.2023.100791](https://doi.org/10.1016/j.jafr.2023.100791).
- 53 H. E. Tahir, L. Zhihua, G. K. Mahunu, *et al.*, Effect of gum arabic edible coating incorporated with African baobab pulp extract on postharvest quality of cold stored blueberries, *Food Sci. Biotechnol.*, 2020, **29**(2), 217–226, DOI: [10.1007/s10068-019-00659-9](https://doi.org/10.1007/s10068-019-00659-9).
- 54 R. Liang, S. Xu, C. F. Shoemaker, Y. Li, F. Zhong and Q. Huang, Physical and Antimicrobial Properties of Peppermint Oil Nanoemulsions, *J. Agric. Food Chem.*, 2012, **60**(30), 7548–7555, DOI: [10.1021/jf301129k](https://doi.org/10.1021/jf301129k).
- 55 N. Nehal, B. Nabi, S. Rehman, *et al.*, Chitosan coated synergistically engineered nanoemulsion of Ropinirole and nigella oil in the management of Parkinson's disease: Formulation perspective and In vitro and In vivo assessment, *Int. J. Biol. Macromol.*, 2021, **167**, 605–619, DOI: [10.1016/j.ijbiomac.2020.11.207](https://doi.org/10.1016/j.ijbiomac.2020.11.207).
- 56 R. Severino, K. D. Vu, F. Donsi, S. Salmieri, G. Ferrari and M. Lacroix, Antibacterial and physical effects of modified chitosan based-coating containing nanoemulsion of mandarin essential oil and three non-thermal treatments against *Listeria innocua* in green beans, *Int. J. Food Microbiol.*, 2014, **191**, 82–88, DOI: [10.1016/j.ijfoodmicro.2014.09.007](https://doi.org/10.1016/j.ijfoodmicro.2014.09.007).
- 57 N. Hasheminejad, F. Khodaiyan and M. Safari, Improving the antifungal activity of clove essential oil encapsulated by chitosan nanoparticles, *Food Chem.*, 2019, **275**, 113–122, DOI: [10.1016/j.foodchem.2018.09.085](https://doi.org/10.1016/j.foodchem.2018.09.085).
- 58 S. Annemer, A. Ez-zoubi, Z. Y. Ez, *et al.*, Optimization and antifungal efficacy against brown rot fungi of combined *Salvia rosmarinus* and *Cedrus atlantica* essential oils encapsulated in Gum Arabic, *Sci. Rep.*, 2023, **13**(1), 19548, DOI: [10.1038/s41598-023-46858-7](https://doi.org/10.1038/s41598-023-46858-7).
- 59 R. L. E. Ayón, Y. G. Uriarte Gastelum, B. H. Camacho Díaz, *et al.*, Antifungal Activity of a Chitosan and Mint Essential Oil Coating on the Development of *Colletotrichum Gloeosporioides* in Papaya Using Macroscopic and Microscopic Analysis, *Food Bioprocess Technol.*, 2022, **15**(2), 368–378, DOI: [10.1007/s11947-022-02764-w](https://doi.org/10.1007/s11947-022-02764-w).
- 60 S. Dos Passos Braga, G. A. Lundgren, S. A. Macedo, *et al.*, Application of coatings formed by chitosan and *Mentha* essential oils to control anthracnose caused by *Colletotrichum gloeosporioides* and *C. brevisporum* in papaya (*Carica papaya* L.) fruit, *Int. J. Biol. Macromol.*, 2019, **139**, 631–639, DOI: [10.1016/j.ijbiomac.2019.08.010](https://doi.org/10.1016/j.ijbiomac.2019.08.010).
- 61 J. Li, I. C. Hwang, X. Chen and H. J. Park, Effects of chitosan coating on curcumin loaded nano-emulsion: Study on stability and in vitro digestibility, *Food Hydrocolloids*, 2016, **60**, 138–147, DOI: [10.1016/j.foodhyd.2016.03.016](https://doi.org/10.1016/j.foodhyd.2016.03.016).
- 62 T. Liu, Z. Gao, W. Zhong, *et al.*, Preparation, Characterization, and Antioxidant Activity of Nanoemulsions Incorporating Lemon Essential Oil, *Antioxidants*, 2022, **11**(4), 650, DOI: [10.3390/antiox11040650](https://doi.org/10.3390/antiox11040650).
- 63 L. Salvia-Trujillo, M. A. Rojas-Graü, R. Soliva-Fortuny and O. Martín-Belloso, Use of antimicrobial nanoemulsions as edible coatings: Impact on safety and quality attributes of fresh-cut Fuji apples, *Postharvest Biol. Technol.*, 2015, **105**, 8–16, DOI: [10.1016/j.postharvbio.2015.03.009](https://doi.org/10.1016/j.postharvbio.2015.03.009).
- 64 M. BenJemaa, F. Z. Rahali, H. Falleh, *et al.*, Essential Oil Stabilisation by Response Surface Methodology (RSM): Nanoemulsion Formulation, Physicochemical, Microbiological, and Sensory Investigations, *Molecules*, 2022, **27**(21), 7330, DOI: [10.3390/molecules27217330](https://doi.org/10.3390/molecules27217330).
- 65 L. C. Sow, F. Tirtawinata, H. Yang, Q. Shao and S. Wang, Carvacrol nanoemulsion combined with acid electrolysed water to inactivate bacteria, yeast in vitro and native microflora on shredded cabbages, *Food Control*, 2017, **76**, 88–95, DOI: [10.1016/j.foodcont.2017.01.007](https://doi.org/10.1016/j.foodcont.2017.01.007).
- 66 F. Chen, M. G. G. M. Kowaleguet, W. Shi, *et al.*, Associating chitosan and nanoemulsion as a delivery system of essential oil; the potential on quality maintenance of minimally processed produce, *LWT*, 2022, **155**, 112925, DOI: [10.1016/j.lwt.2021.112925](https://doi.org/10.1016/j.lwt.2021.112925).
- 67 Y. Ma, P. Liu, K. Ye, *et al.*, Preparation, Characterization, In Vitro Release, and Antibacterial Activity of Oregano Essential Oil Chitosan Nanoparticles, *Foods*, 2022, **11**(23), 3756, DOI: [10.3390/foods11233756](https://doi.org/10.3390/foods11233756).
- 68 C. Cai, R. Ma, M. Duan and D. Lu, Preparation and antimicrobial activity of thyme essential oil microcapsules prepared with gum arabic, *RSC Adv.*, 2019, **9**(34), 19740–19747, DOI: [10.1039/C9RA03323H](https://doi.org/10.1039/C9RA03323H).
- 69 W. Zhang, C. Shu, Q. Chen, J. Cao and W. Jiang, The multi-layer film system improved the release and retention properties of cinnamon essential oil and its application as coating in inhibition to penicillium expansion of apple fruit, *Food Chem.*, 2019, **299**, 125109, DOI: [10.1016/j.foodchem.2019.125109](https://doi.org/10.1016/j.foodchem.2019.125109).
- 70 Y. A. Oh, Y. J. Oh, A. Y. Song, J. S. Won, K. B. Song and S. C. Min, Comparison of effectiveness of edible coatings using emulsions containing lemongrass oil of different size droplets on grape berry safety and preservation, *LWT*, 2017, **75**, 742–750, DOI: [10.1016/j.lwt.2016.10.033](https://doi.org/10.1016/j.lwt.2016.10.033).
- 71 V. Gupta, R. Yadav, R. Tanwar and K. K. Gaikwad,  $\kappa$ -Carrageenan-based bio-nanocomposite film reinforced with cellulose nanocrystals derived from amla pomace for



- food packaging, *Biomass Convers. Biorefin.*, 2021, **13**, 16899–16908, DOI: [10.1007/s13399-021-02028-1](https://doi.org/10.1007/s13399-021-02028-1).
- 72 I. H. Kim, Y. A. Oh, H. Lee, K. B. Song and S. C. Min, Grape berry coatings of lemongrass oil-incorporating nanoemulsion, *LWT–Food Sci. Technol.*, 2014, **58**(1), 1–10, DOI: [10.1016/j.lwt.2014.03.018](https://doi.org/10.1016/j.lwt.2014.03.018).
- 73 I. Dammak and P. José Do Amaral Sobral, Formulation optimization of lecithin-enhanced pickering emulsions stabilized by chitosan nanoparticles for hesperidin encapsulation, *J. Food Eng.*, 2018, **229**, 2–11, DOI: [10.1016/j.jfoodeng.2017.11.001](https://doi.org/10.1016/j.jfoodeng.2017.11.001).
- 74 C. Diedrich, I. C. Zittlau, N. M. Khalil, *et al.*, Optimized Chitosan-Based Nanoemulsion Improves Luteolin Release, *Pharmaceutics*, 2023, **15**(6), 1592, DOI: [10.3390/pharmaceutics15061592](https://doi.org/10.3390/pharmaceutics15061592).
- 75 A. Parven, M. R. Sarker, M. Megharaj and I. M. Meftaul, Prolonging the shelf life of Papaya (*Carica papaya* L.) using Aloe vera gel at ambient temperature, *Sci. Hortic.*, 2020, **265**, 109228, DOI: [10.1016/j.scienta.2020.109228](https://doi.org/10.1016/j.scienta.2020.109228).
- 76 F. Rashid, Z. Ahmed, K. Ameer, R. M. Amir and M. Khattak, Optimization of polysaccharides-based nanoemulsion using response surface methodology and application to improve postharvest storage of apple (*Malus domestica*), *J. Food Meas. Charact.*, 2020, **14**(5), 2676–2688, DOI: [10.1007/s11694-020-00514-0](https://doi.org/10.1007/s11694-020-00514-0).
- 77 A. Ali, G. K. Hei and Y. W. Keat, Efficacy of ginger oil and extract combined with gum arabic on anthracnose and quality of papaya fruit during cold storage, *J. Food Sci. Technol.*, 2016, **53**(3), 1435–1444, DOI: [10.1007/s13197-015-2124-5](https://doi.org/10.1007/s13197-015-2124-5).
- 78 M. Radi, S. Akhavan-Darabi, H. Akhavan and S. Amiri, The use of orange peel essential oil microemulsion and nanoemulsion in pectin-based coating to extend the shelf life of fresh-cut orange, *J. Food Process. Preserv.*, 2018, **42**(2), e13441, DOI: [10.1111/jfpp.13441](https://doi.org/10.1111/jfpp.13441).
- 79 S. Manzoor, A. Gull, S. M. Wani, *et al.*, Improving the shelf life of fresh cut kiwi using nanoemulsion coatings with antioxidant and antimicrobial agents, *Food Biosci.*, 2021, **41**, 101015, DOI: [10.1016/j.fbio.2021.101015](https://doi.org/10.1016/j.fbio.2021.101015).
- 80 M. C. Yu, C. Y. Hou, C. W. Hsieh, J. S. Tsay, H. Y. Chung and Y. S. Liang, Effects of D-Limonene Nanoemulsion Coating on Post-Harvest Quality and Physiology of Papaya, *Horticulturae*, 2023, **9**(9), 975, DOI: [10.3390/horticulturae9090975](https://doi.org/10.3390/horticulturae9090975).
- 81 N. Robledo, L. López, A. Bungler, C. Tapia and L. Abugoch, Effects of Antimicrobial Edible Coating of Thymol Nanoemulsion/Quinoa Protein/Chitosan on the Safety, Sensorial Properties, and Quality of Refrigerated Strawberries (*Fragaria* × *ananassa*) Under Commercial Storage Environment, *Food Bioprocess Technol.*, 2018, **11**(8), 1566–1574, DOI: [10.1007/s11947-018-2124-3](https://doi.org/10.1007/s11947-018-2124-3).
- 82 A. Prakash, R. Baskaran and V. Vadivel, Citral nanoemulsion incorporated edible coating to extend the shelf life of fresh cut pineapples, *LWT*, 2020, **118**, 108851, DOI: [10.1016/j.lwt.2019.108851](https://doi.org/10.1016/j.lwt.2019.108851).
- 83 M. Zhou, J. Ma, Y. Yi, *et al.*, Chitosan-Based Edible Coating Containing Ascorbic Acid/Curcumin for Improving Postharvest Quality and Storability of Strawberry Fruits, *J. Future Foods*, 2025, S2772566925004306, DOI: [10.1016/j.jfutfo.2025.10.039](https://doi.org/10.1016/j.jfutfo.2025.10.039).
- 84 V. K. Pandey, R. U. Islam, R. Shams and A. H. Dar, A comprehensive review on the application of essential oils as bioactive compounds in Nano-emulsion based edible coatings of fruits and vegetables, *Appl. Food Res.*, 2022, **2**(1), 100042, DOI: [10.1016/j.afres.2022.100042](https://doi.org/10.1016/j.afres.2022.100042).
- 85 S. Showkat, N. Anjum, Q. Ayaz, *et al.*, Enhancing shelflife of plum fruit by chitosan-based nanoemulsion coating incorporated with ginger essential oil, *Appl. Food Res.*, 2025, **5**(1), 100768, DOI: [10.1016/j.afres.2025.100768](https://doi.org/10.1016/j.afres.2025.100768).
- 86 S. Z. Iqbal, M. Waseem, F. Naz, *et al.*, Application of Chitosan and Pectin-Based Nanoemulsion Coating for the Preservation of Plum (*Prunus domestica*) Fruit, *Food Sci. Nutr.*, 2025, **13**(9), e70824, DOI: [10.1002/fsn3.70824](https://doi.org/10.1002/fsn3.70824).
- 87 Q. D. Nguyen, Q. D. Pham and A. D. Do, Characterization of a chitosan-based nanoemulsion loaded with Niaouli (*Melaleuca quinquenervia*) essential oil and its effect on postharvest fungi and ripening of banana fruit, *Eur. Food Res. Technol.*, 2026, **252**(1), 16, DOI: [10.1007/s00217-025-05006-3](https://doi.org/10.1007/s00217-025-05006-3).
- 88 M. Miranda, M. D. M. M. Ribeiro, P. C. Spricigo, *et al.*, Carnauba wax nanoemulsion applied as an edible coating on fresh tomato for postharvest quality evaluation, *Heliyon*, 2022, **8**(7), e09803, DOI: [10.1016/j.heliyon.2022.e09803](https://doi.org/10.1016/j.heliyon.2022.e09803).

